

Sandia National Laboratories

53rd annual meeting of the APS Division of Plasma Physics
Salt Lake City, UT
November 14 – 18, 2011

Investigating ICF target fuel conditions through x-ray spectroscopy

Stephanie Hansen

Sandia National Laboratories, Albuquerque, NM 87185 USA

With thanks to: D. Ampleford, J. Bailey, G. Dunham, M. Herrmann,
C. Jennings, B. Jones, C. Nakhleh, K. Peterson, G. Rochau,
D. Sinars, S. Slutz, R. Vesey, E. Yu, (SNL) H. Scott, and B. Wilson (LLNL)



Sandia is a multiprogram laboratory operated by Sandia Corporation, a Lockheed Martin Company, for the United States Department of Energy's National Nuclear Security Administration under contract DE-AC04-94AL85000.



Sandia National Laboratories

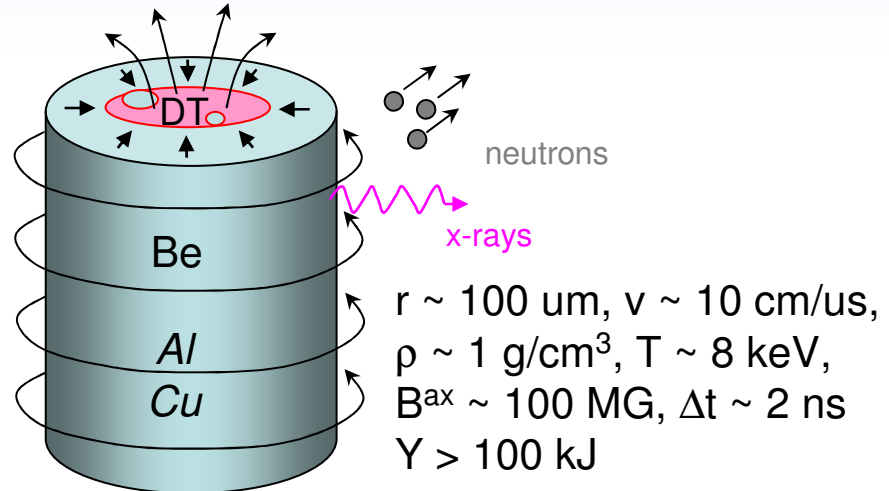


Outline

- We are developing diagnostic strategies for a magnetized ICF plasma concept, MagLIF [1]

- increase v , p , & Y
- decrease Δt & (B)

} \rightarrow NIF [2]



- While neutron yields are the bottom line in ICF, x-ray spectroscopy can be a powerful complement to neutron diagnostics. We are leveraging a strong history of spectroscopy on Z:
 - extensive instrumental capabilities
 - advanced theoretical atomic modeling (LLNL & SNL)
 - new radiation transport & post-processing capabilities
- A tale of two plasmas:
 - similar neutron signals
 - profoundly different x-ray spectra

1. S.A. Slutz *et al.*, Phys Plas **17**, 056303 (2010)
2. J.D. Lindl *et al.*, Phys Plas **11**, 339 (2004)

Z has extensive spectroscopic instrumentation

We routinely field up to eight spectrometers per shot, spanning the spectral range 1 – 20 keV with $\epsilon/\Delta\epsilon \sim 1000$



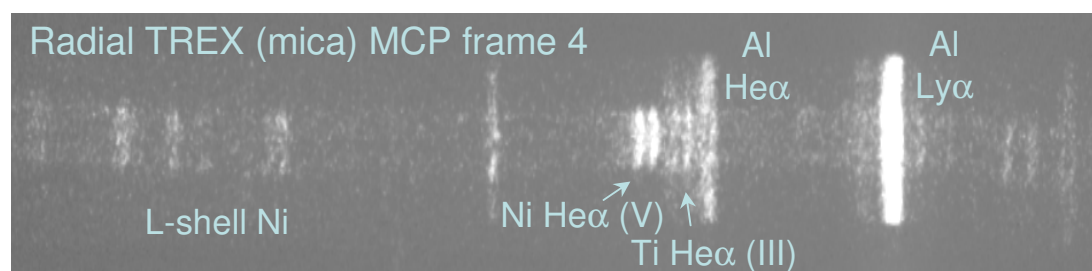
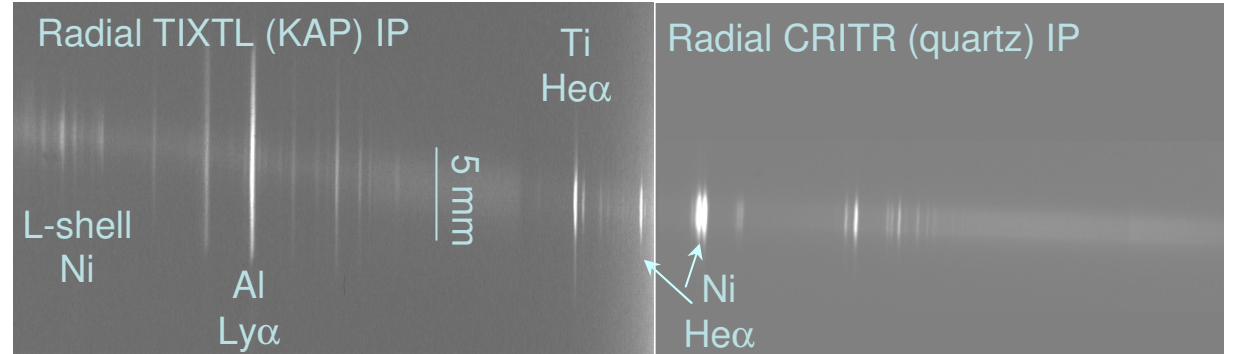
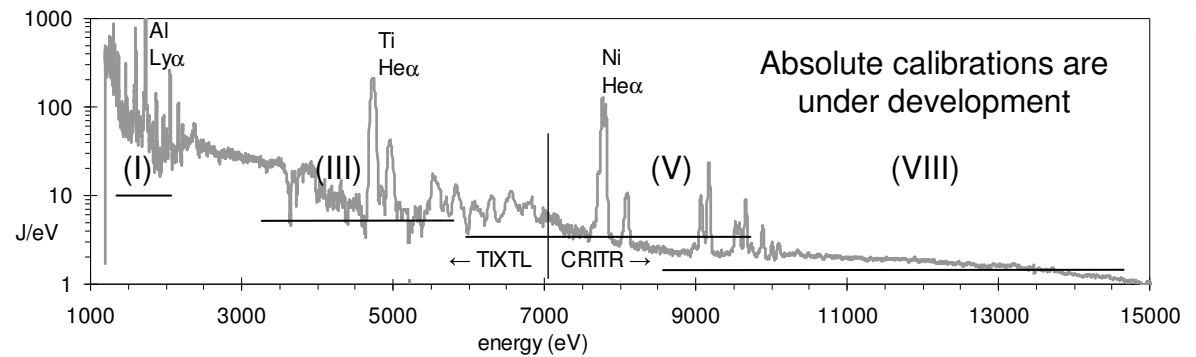
(4) TREX³ / PODD⁴
1-D space res. (50 – 300 μm)
time-gated (~ 0.5 ns)

(4) TREX⁵ / TIXTL
1-D space res.
time-gated + time-int



source

(2) CRITR⁶
1-D space res. (~ 80 μm)
time-integrated



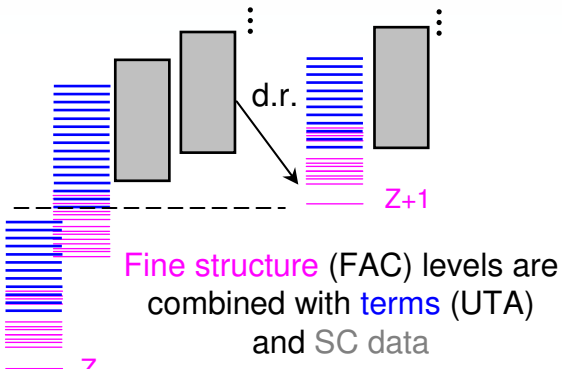
Spatial, temporal, and spectral resolution are all important.

3. Bailey *et al.*, PRL **99**, 265002 (2007).
4. Gomez, Rochau, *et al.*, (in prep)

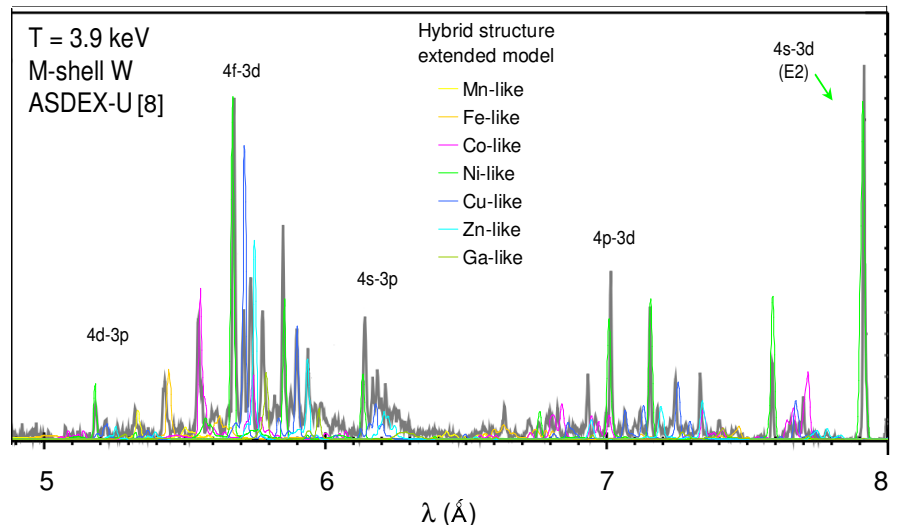
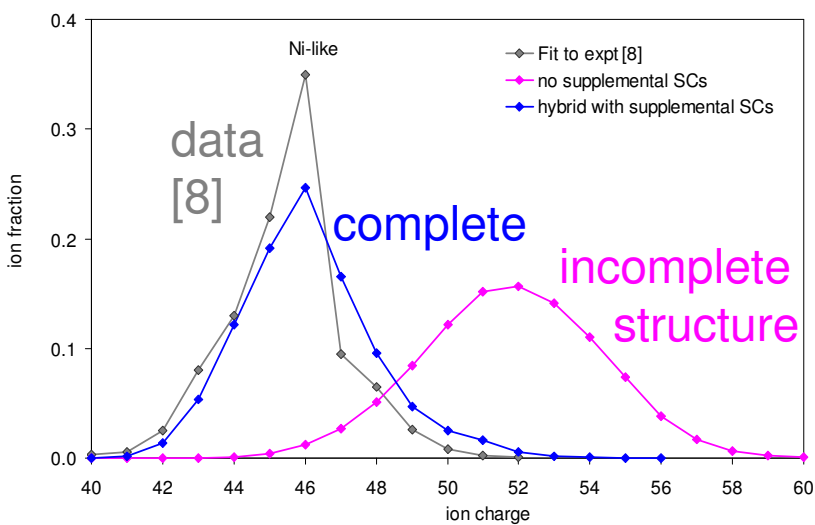
5. Lake *et al.*, RSI **75**, 3690 (2004).
6. Sinars *et al.*, RSI **82**, 063113 (2011).

We have developed reliable non-LTE atomic models with spectroscopic accuracy

Hybrid level structure [7] ensures statistical completeness in high- n states, multiply excited states, and d.r. channels...



... while retaining spectroscopic accuracy in resonance lines, important satellite features, and emission from metastable states.

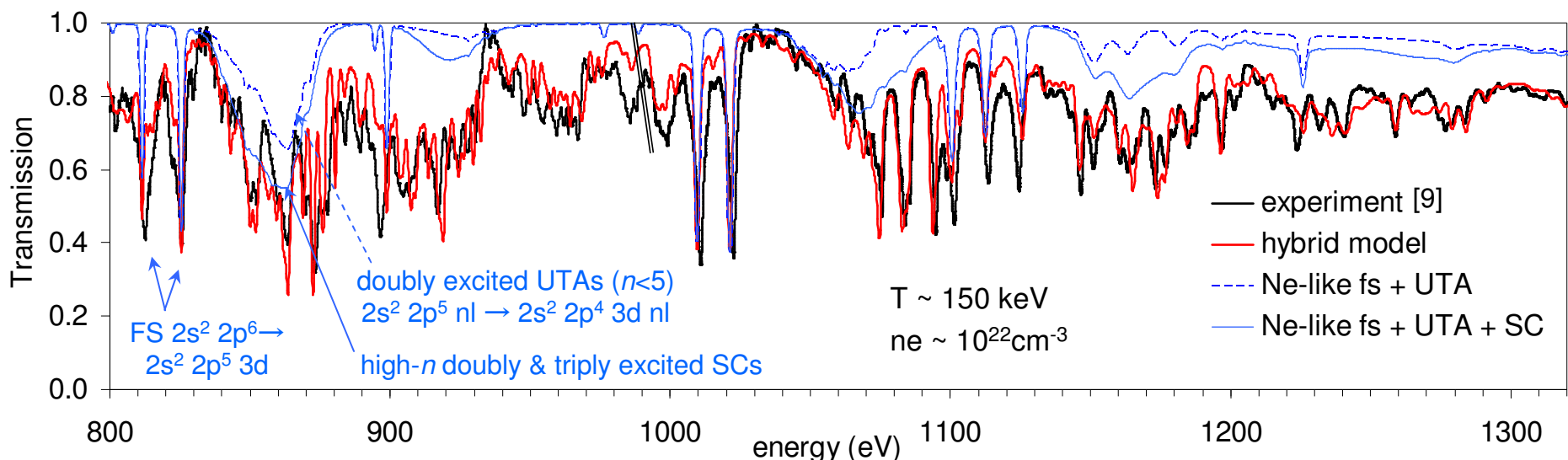


To keep things tractable, we only model in detail what can be measured in detail

7. Hansen, Bauche, Bauche-Arnoult, and Gu, HEDP **3**, 109 (2007); Hansen Can. J. Phys **89**, 633 (2011)
 8. Pütterich et al. Plasma Phys. Control. Fusion **50**, 085016 (2008)

At the extreme conditions of interest to ICF, multiple density effects must be included

- Stark and collisional effects lead to line broadening and shifting
- The substantial “sea” of free electrons weakens the binding of high- n electrons, leading to continuum lowering and plasma polarization line shifts
- with increasing collisionality, multiply excited states can dominate the populations, resulting in an explosion of statistical weight even as the number of bound orbitals decrease

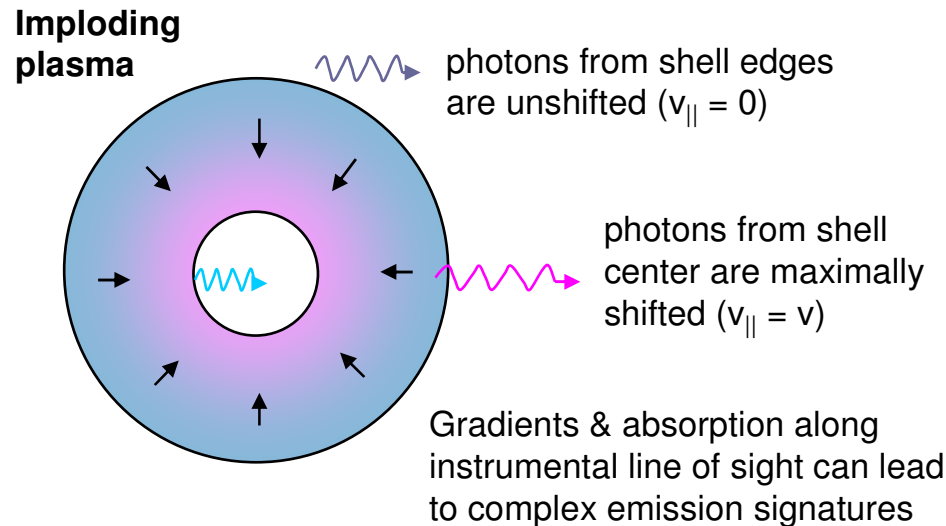


Fine structure lines, UTAs, and supplemental SCs [10] all contribute to good data fit with only $\sim 10^5$ lines (vs. $> 10^7$ for a fully fine structure model)

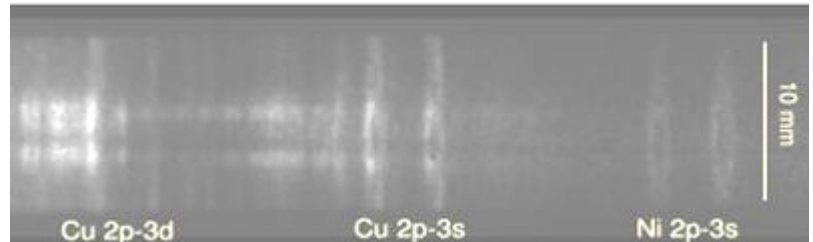
9. Bailey *et al.* PRL **99**, 265002 (2007).

10. Scott & Hansen, HEDP **6**, 39 (2010). (Wilson/Albritton data for UTAs)

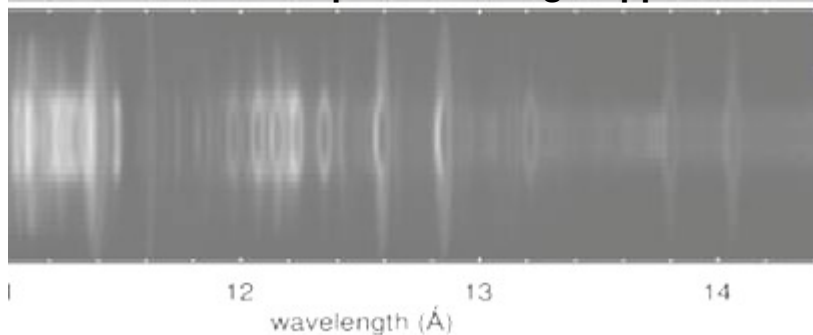
A good atomic model is not enough: self-consistent radiation transport is critical



Time-gated, radially resolved expt. spectrum



Model with full transport including Doppler effects



We are developing a tabular, iterative on-the-spot approach that fully integrates Doppler effects, determining self-consistent emissivities using 3-D ray tracing in Cartesian geometry and generating spatially resolved line profiles for ions and mixtures of arbitrary complexity [11].

Self-consistent transport is important both for diagnostics based on simple plasma models and for post-processing simulations

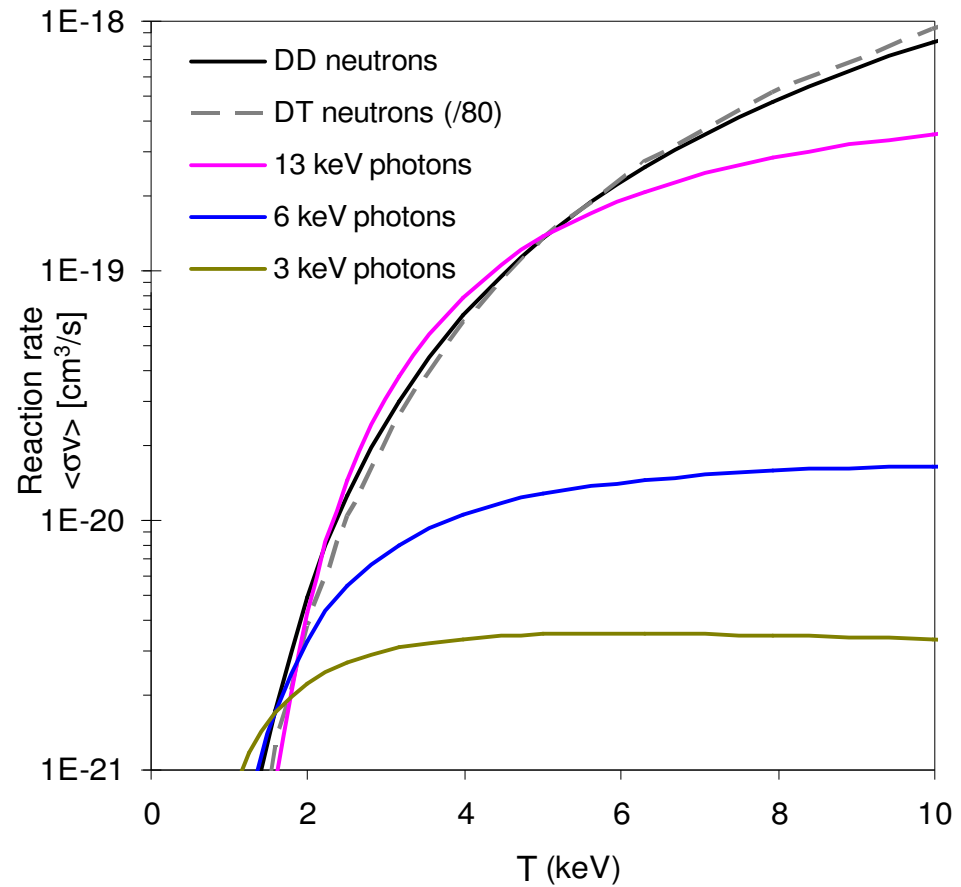
These x-ray spectroscopy capabilities complement neutron data for ICF plasmas

Neutron yields alone are indiscriminate:

$$R = n_T n_D \langle \sigma_{DT} v_{ion}(T) \rangle \text{Vol} \text{ [n/s]}$$

A given neutron yield can be generated by a multiplicity of burn plasmas whose density, volume, temperature and duration satisfy $Y = R\Delta t$

More extensive neutron diagnostics can constrain ρr and T_{ion} , but they do not (easily) reveal gradients, mix, B...



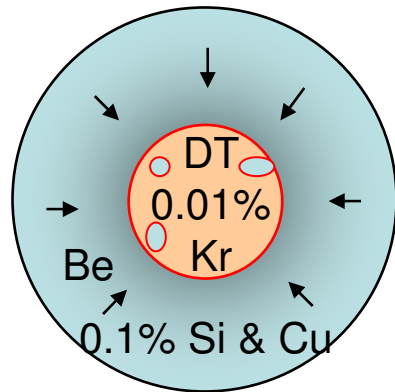
High-energy x-rays (> 10 keV) of dopants co-located with the fusion fuel [12] are reasonable neutron proxies

Consider two fusion plasmas with identical yields:

For both, the neutron diagnostics suggest $\rho_r \sim 0.5 \text{ g/cm}^2$ and $T_{\text{ion}} \sim 8 \text{ keV}$;
but the measured yield was a factor of 10 lower than expected.

Case 1

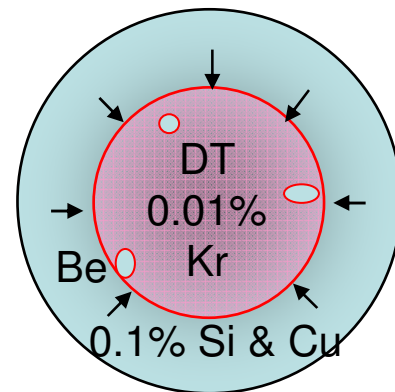
$\rho \sim 100 \text{ g/cc}$ (nominal)
 $r \sim 50 \text{ um}$ (nominal)
 $T_{\text{ion}} \sim 3.5 \text{ keV}$ (low!)



Fuel was incompletely thermalized;
residual $v \sim 30 \text{ cm/us}$ broadened NTOF [13]

Case 2

$\rho \sim 10 \text{ g/cc}$ (low!)
 $r \sim 100 \text{ um}$ (~high)
 $T_{\text{ion}} \sim 8 \text{ keV}$ (nominal)

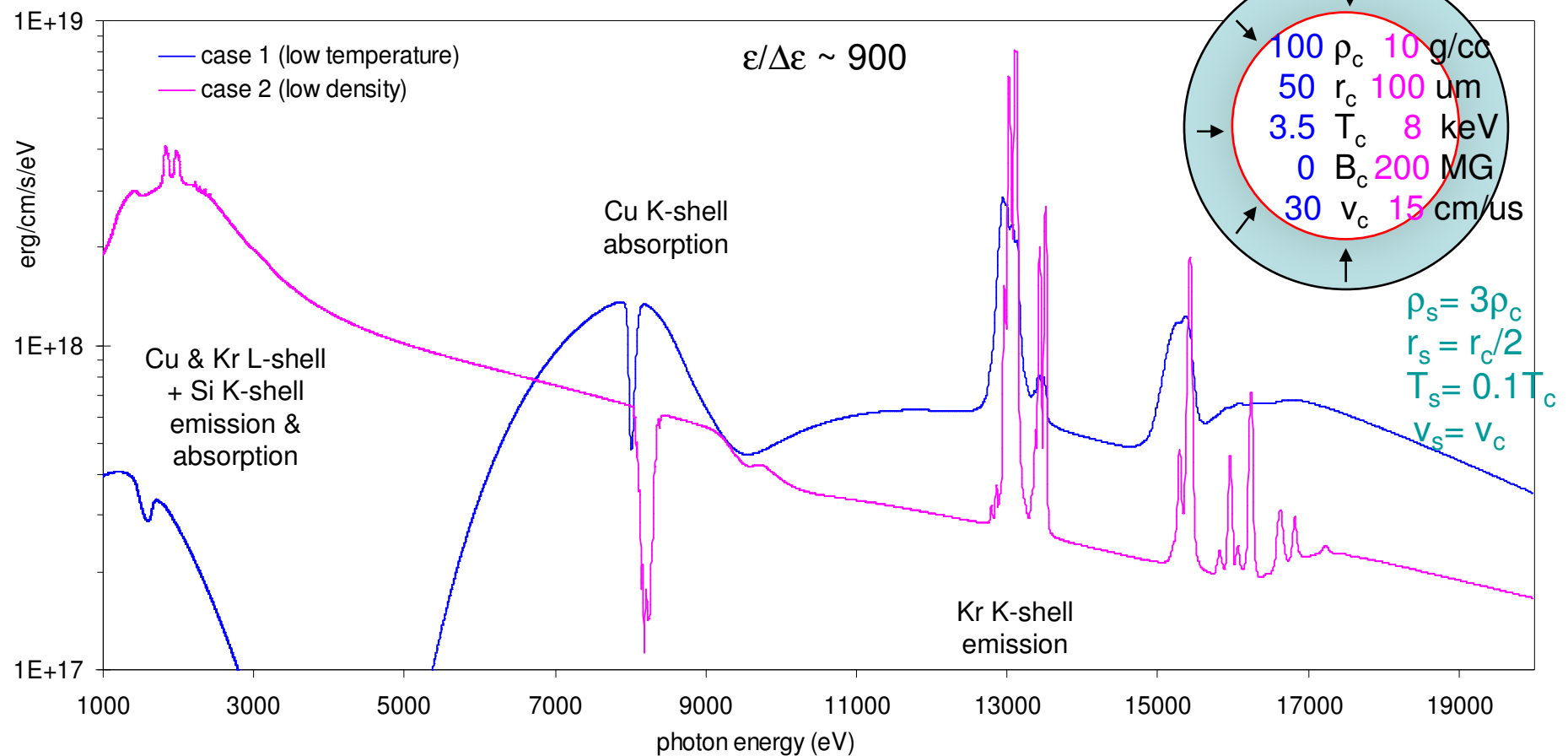


$B \sim 2 \times 10^4 \text{ T}$ increased secondary
DT neutron production

Even fusion plasmas that have similar yields, burn durations, and neutron signatures can underperform for very different reasons.

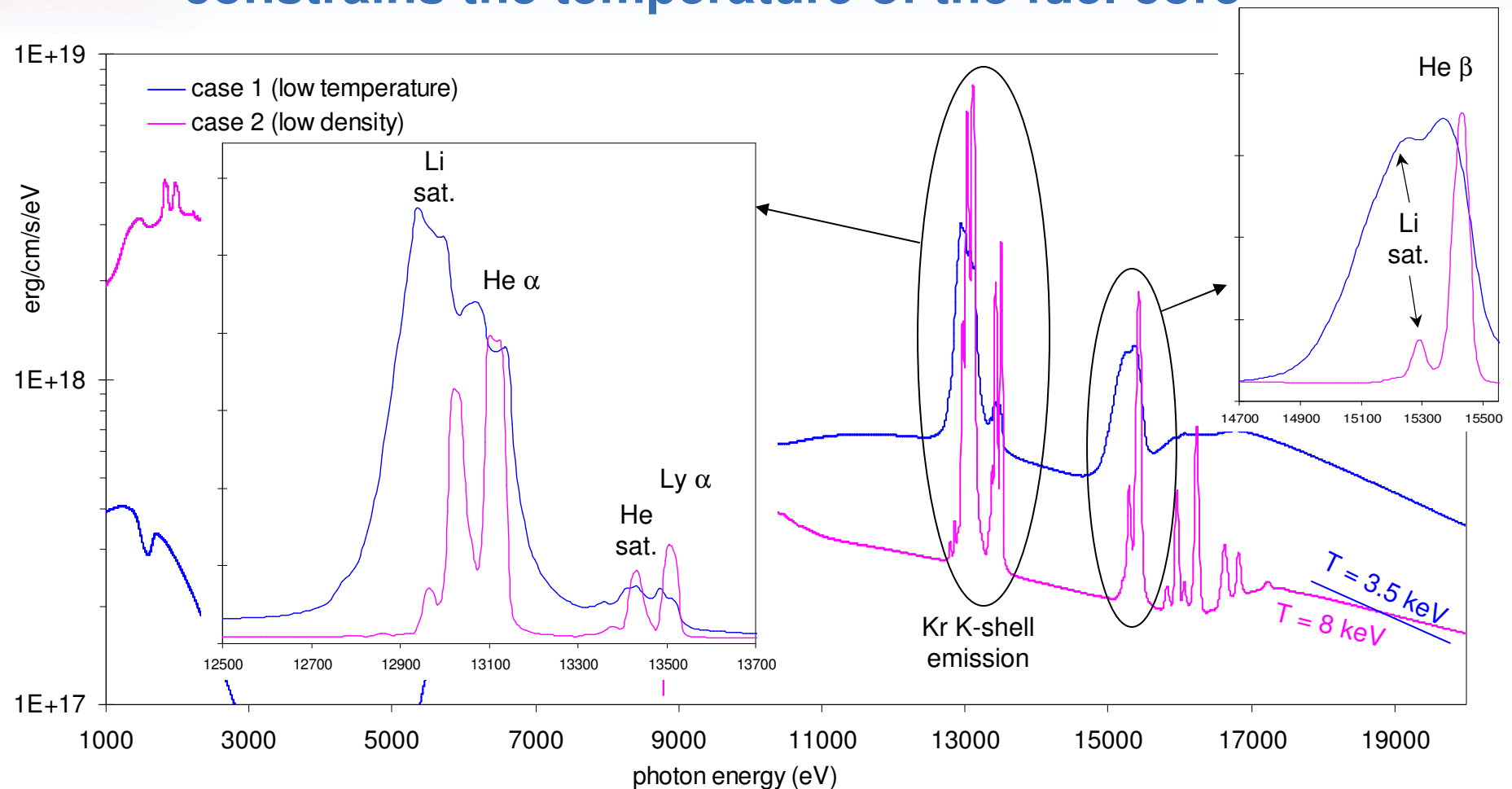
How would we know?

The emitted x-ray spectra are dramatically different



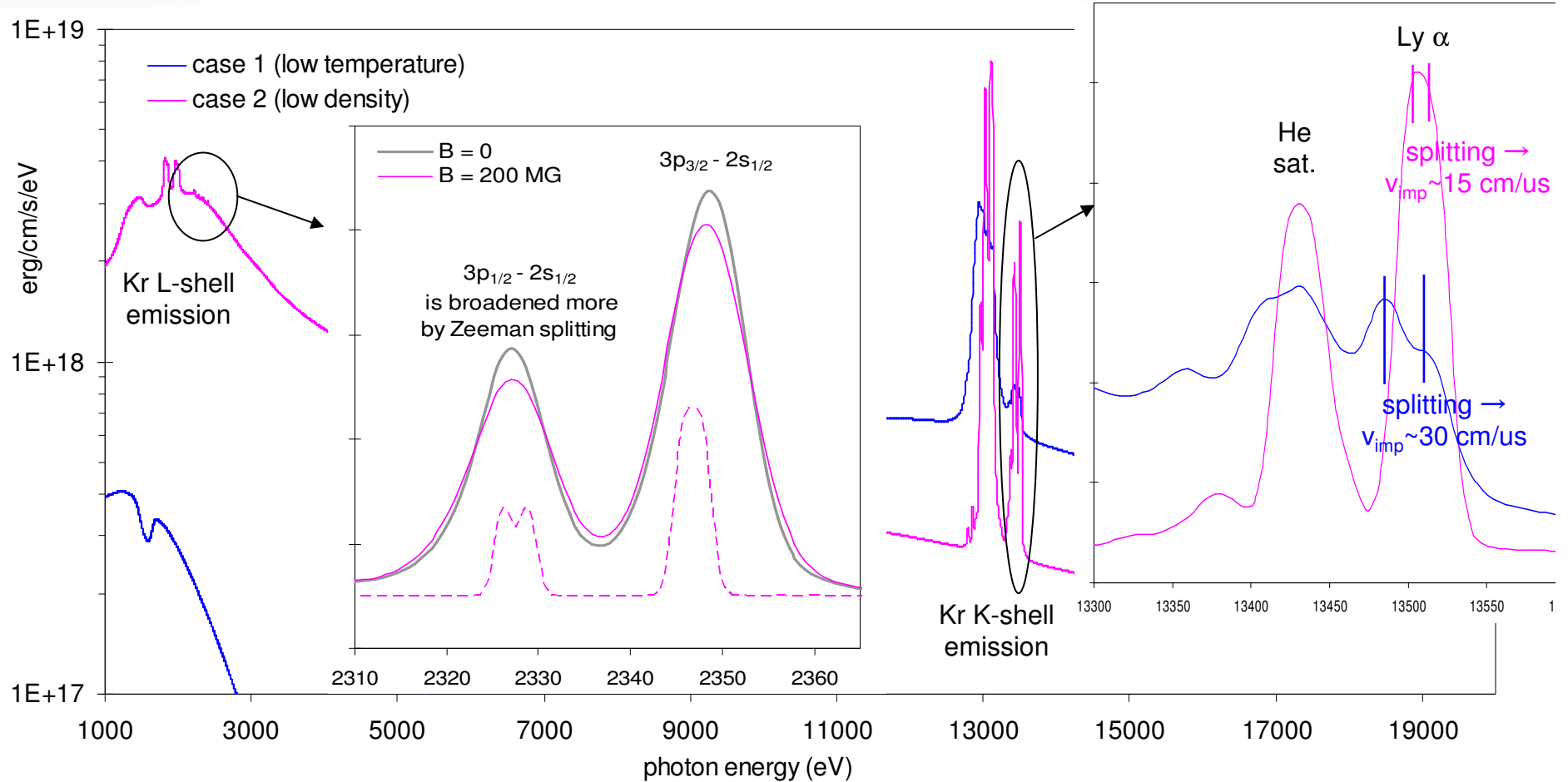
There are profound differences in the widths of emission & absorption features, emission line ratios, and the depth and position of absorption lines.

High-energy photon emission constrains the temperature of the fuel core



Absent strong absorption, continuum slope and line ratios are good thermometers.
Opacity effects in the α features can inform pr.

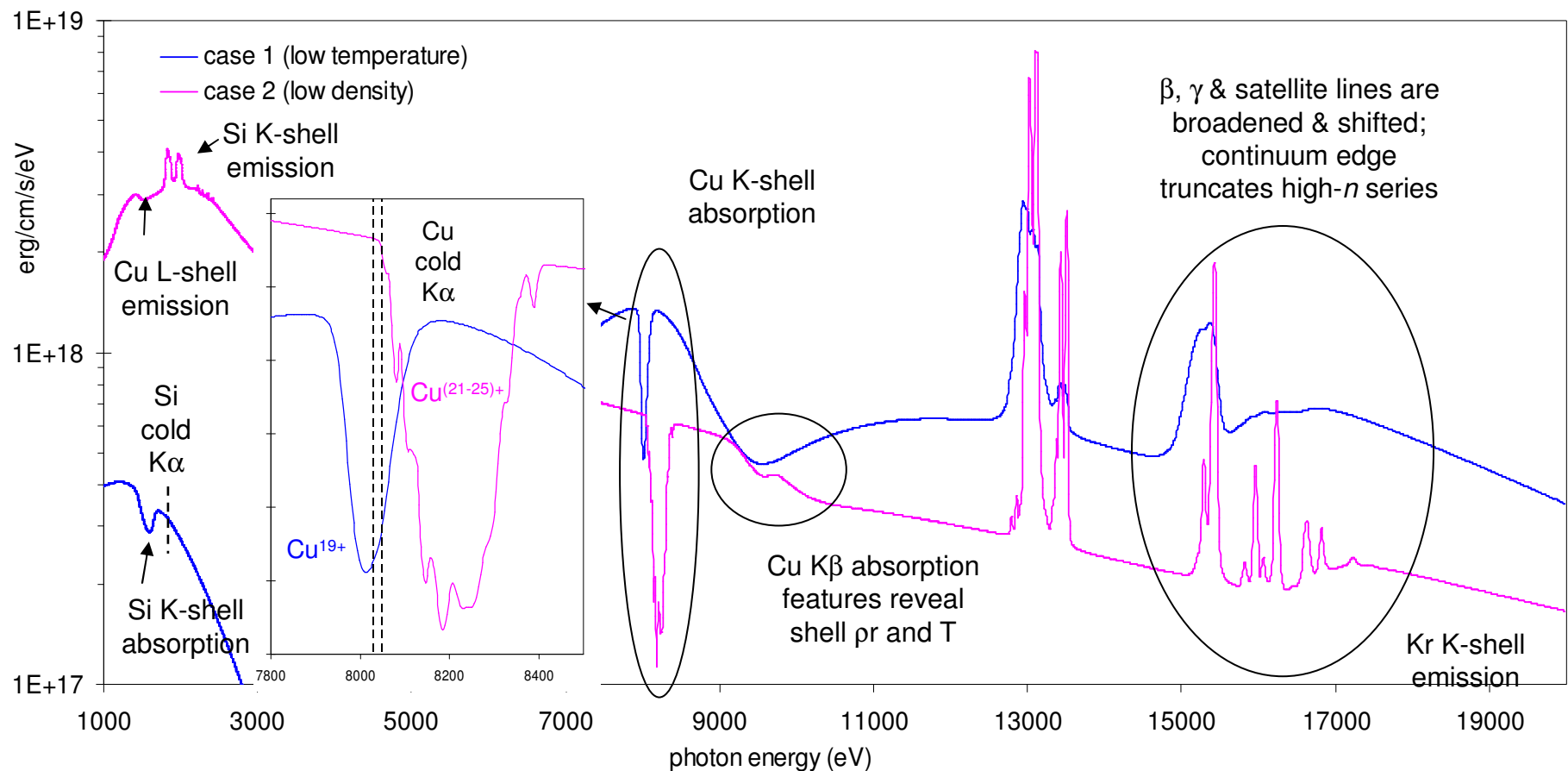
~Optically thin lines can reveal information about implosion velocities and magnetic fields ¹⁴



A naïve reading of neutron data might overestimate case 1 T and case 2 pr. Motional and Zeeman broadening could also lead to an overestimate of density from the x-ray emission.

14. Stambulchik, Tsigutkin, and Maron, PRL **98**, 225001 (2007)

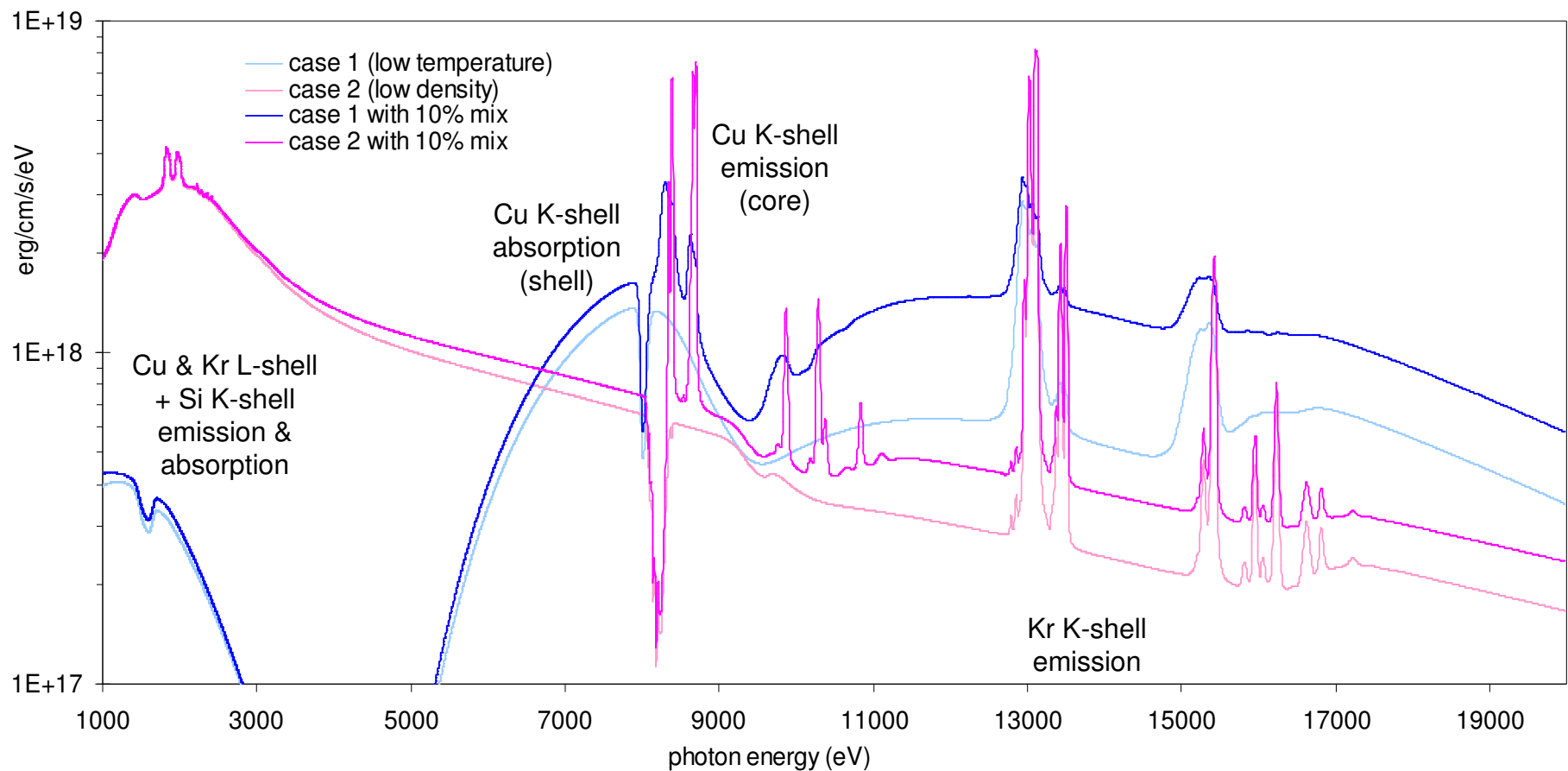
Densities in core and shell can be assessed by continuum lowering and plasma polarization ¹⁵



These effects are distinguishable from other broadening mechanisms. Ultrahigh densities are the *only* way to produce absorption or emission below cold K α (Both Stark and plasma polarization shifts must be modeled).

15. Nguyen, Koenig, Benredjem, Caby, and Coulaud, PRA **33**, 1279 (1986).

Mixing of shell dopants into fuel has profound effects on the emission



If mix is confined neatly to fuel edges, temperature and density gradients can be determined by analyzing Cu (Ge) emission features just as we did for Kr. Localized dopants can provide additional spatial resolution.

Mixing of Ge-doped CH has been observed on NIF

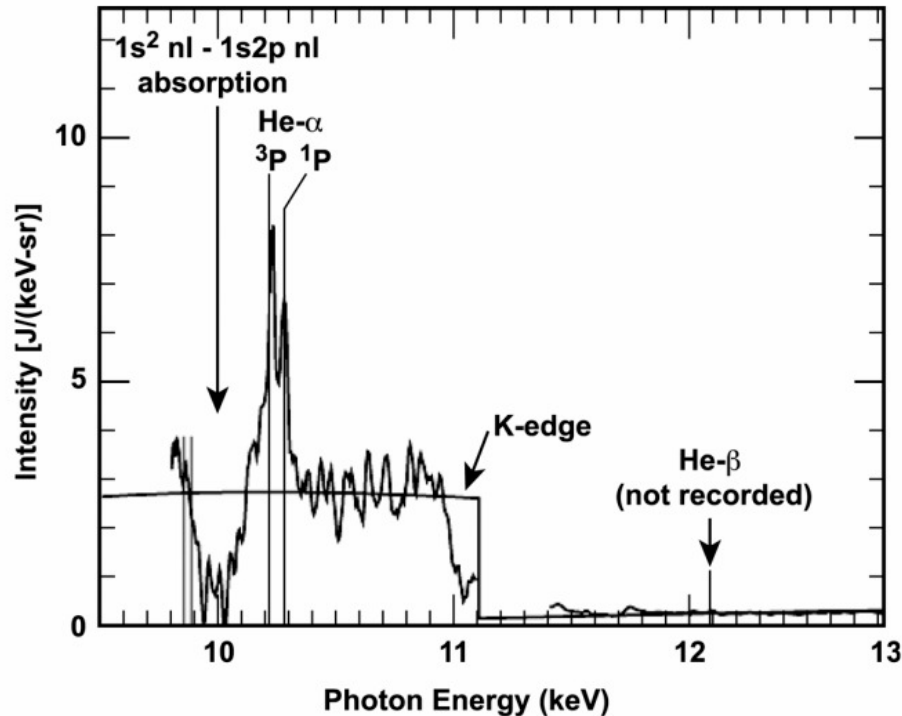


FIG. 12. X-ray spectra from absolutely calibrated x-ray spectrometer, recorded on 1.3 MJ Rev 5 Symcap implosion (Fall 2010) showing Ge He- α at ~ 10.25 keV (resonance $[{}^1\text{P}-{}^1\text{S}]$ and intercombination $[{}^3\text{P}-{}^1\text{S}]$), clear evidence that Ge has entered the hot-spot. The cold Ge in the surrounding shell results in 1s^2 nl- $1\text{s}2\text{p}$ nl absorption on the low energy side of He- α , and absorption above the Ge K-edge which strongly attenuates He- β and the free-bound ($f-b$) continuum. Spectrum is integrated over the full spatial extent of the emitting compressed core.

From Hammel, Scott, Regan *et al.*, Phys Plas **18**, 056310 (2011).

Hammel, Scott, Regan *et al.* [Phys Plas **18**, 056310 (2011)] have measured & analyzed Ge K-shell emission & absorption from jets of ablator material, determining $(T, \rho)_{\text{fuel}}$, $(T, \rho_r)_{\text{shell}}$, and estimating the mass of entrained ablator material.

Future NIC experiments will include Si (Cu, Zn) doped layers to reduce cold Ge opacity and add spatial resolution.

With Br/Kr dopant in the fuel, additional data on the fusion plasma and its gradients could be obtained.

Measuring Si K/Ge(Cu) L might inform shell velocities & ρ

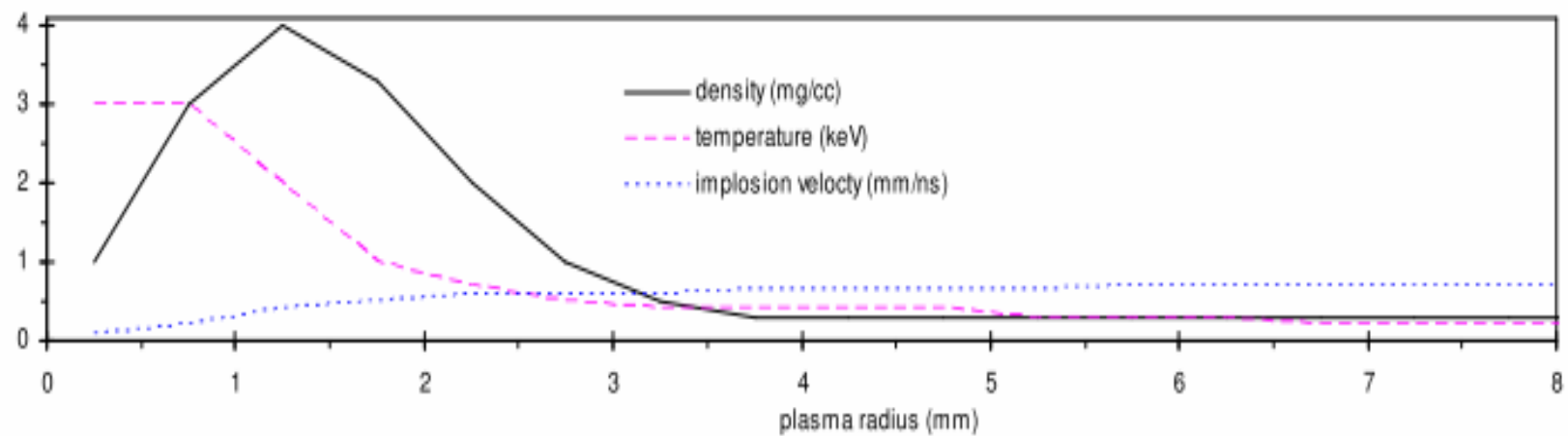


Conclusions

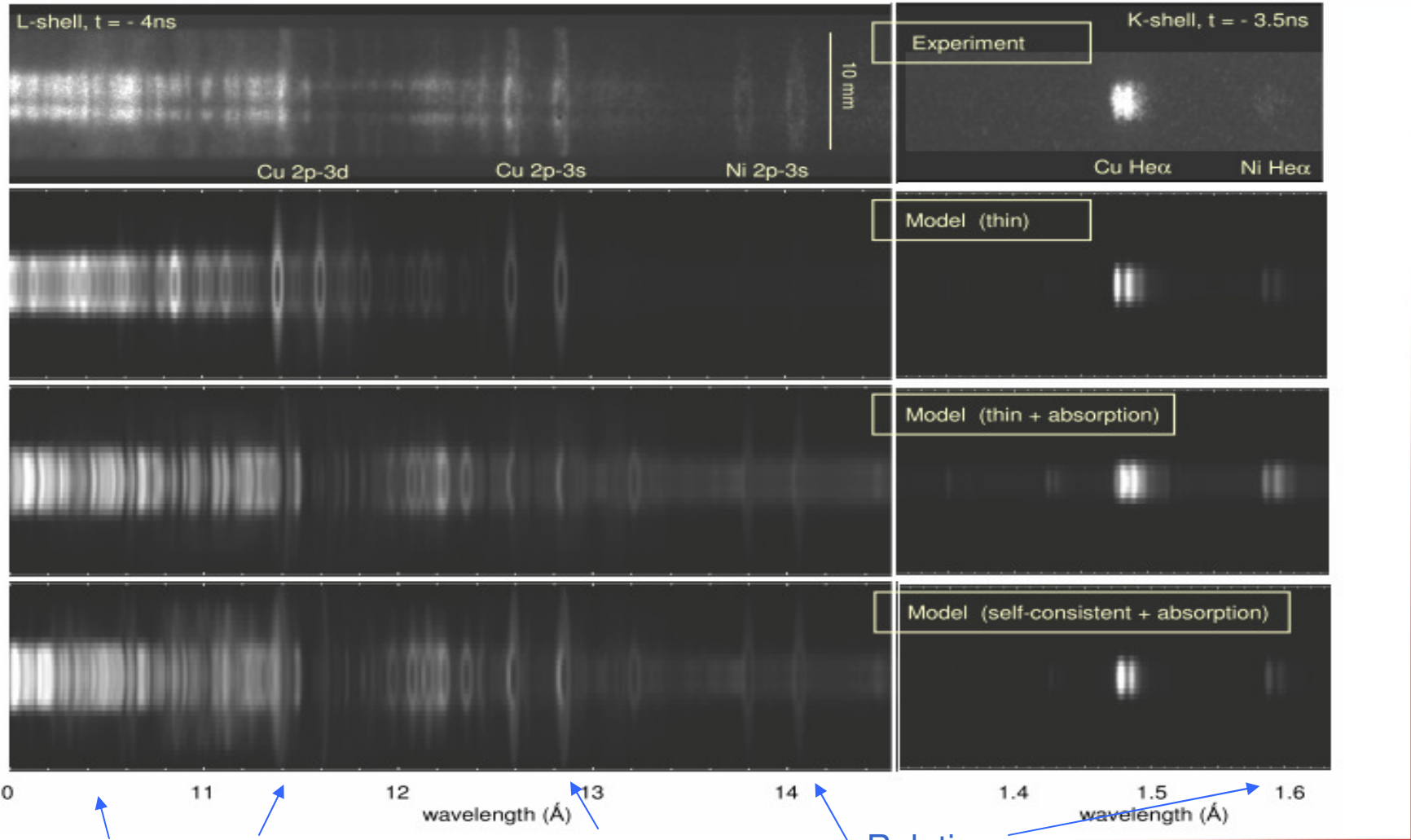
- **X-ray spectroscopy is a powerful diagnostic:**
 - Emission signatures in x-ray spectra tell us about the temperatures, densities, ρr , velocities, fields and mix in the hot cores of ICF plasmas
 - Absorption signatures tell us about temperature & density gradients and ρr of the pusher
 - Spectroscopy can resolve ambiguities in neutron data and provide strong diagnostic data to help constrain simulations
- **The tools required to exploit x-ray emission from ICF plasmas include:**
 - instrumental capabilities to see a large range of photon energies with adequate spatial, temporal, and spectral resolution
 - advanced, spectroscopically accurate non-LTE atomic models reliable at arbitrary densities
 - post-processing capabilities that can account for motional Doppler shifts, self-consistent photopumping (including fluorescence), and which can generate simulated diagnostic data for comparison with experiment



Diagnosed density, temperature, and velocity profiles

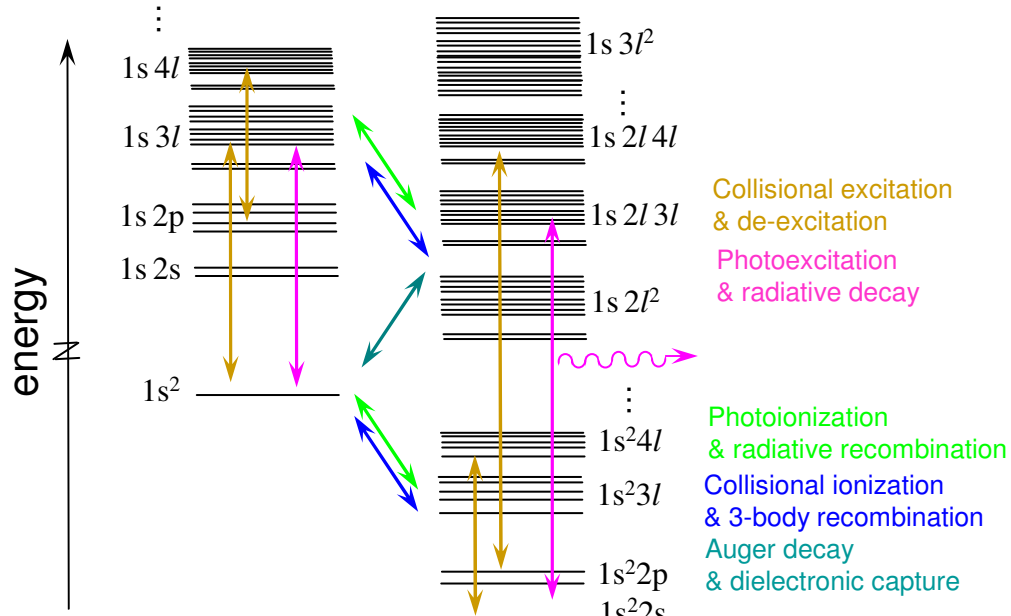


With full transport and tabulated model, we can reproduce the major features of multiply resolved data



Collisional-radiative models: atomic levels (states) coupled by atomic processes (rates)

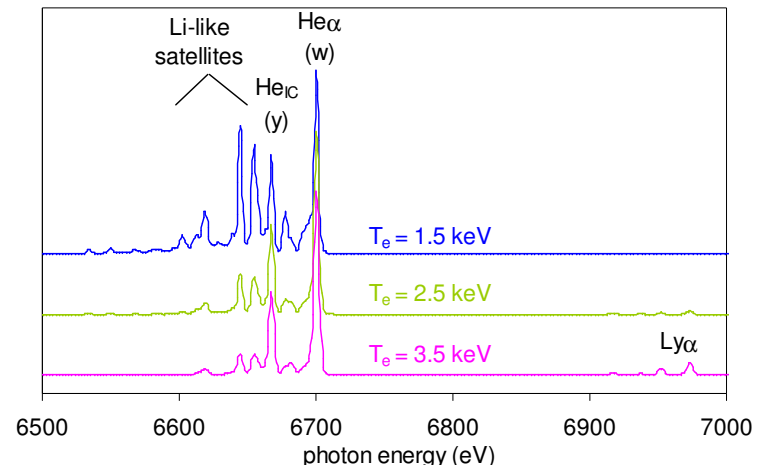
Example: He- and Li-like ions



A variety of codes, (RATS, FAC, Cowan...), databases, (NIST, ATOMDB...), and approximations (screened hydrogenic, Lotz...) provide energy level structure and rate data – with varied accuracy.

Collisional and spontaneous rates form a rate matrix that is inverted to determine level populations.

With populations and radiative rates, synthetic spectra can be constructed and used for plasma diagnostics or radiation-hydrodynamic simulations

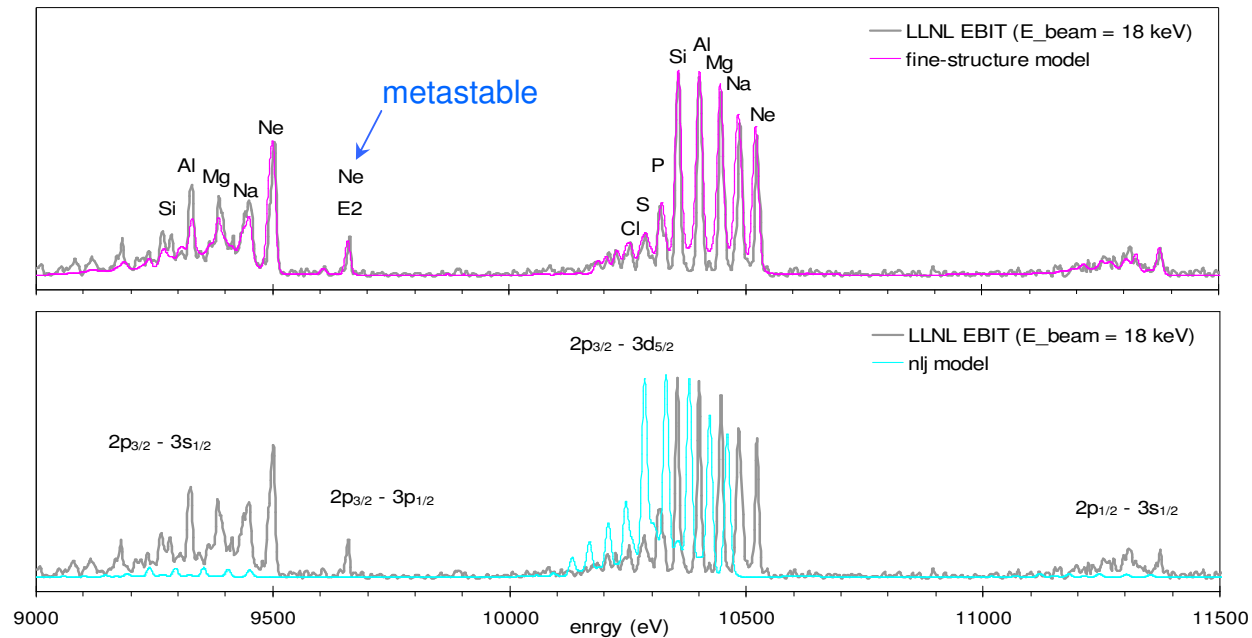


Example: K-shell Fe emission spectra

Low-density “coronal” models generally use high-accuracy atomic data

Coronal atomic models are widely used for EBIT, tokamak, and astrophysical sources, where low densities ensure that population is concentrated in ground states

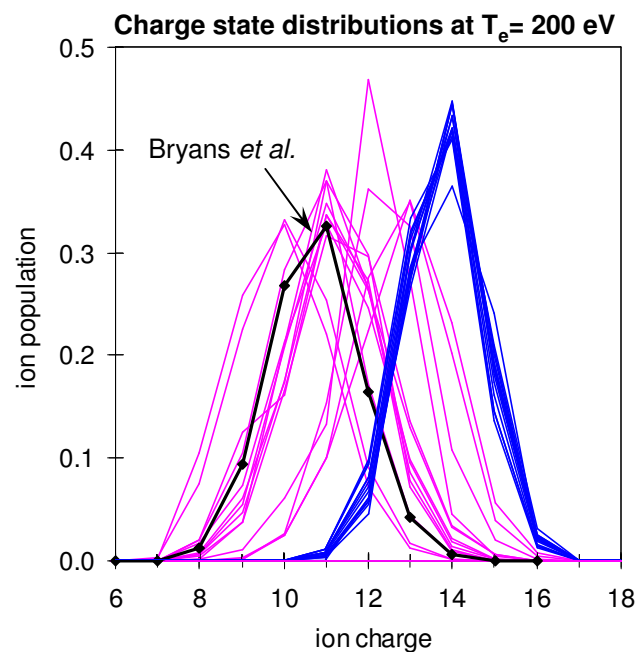
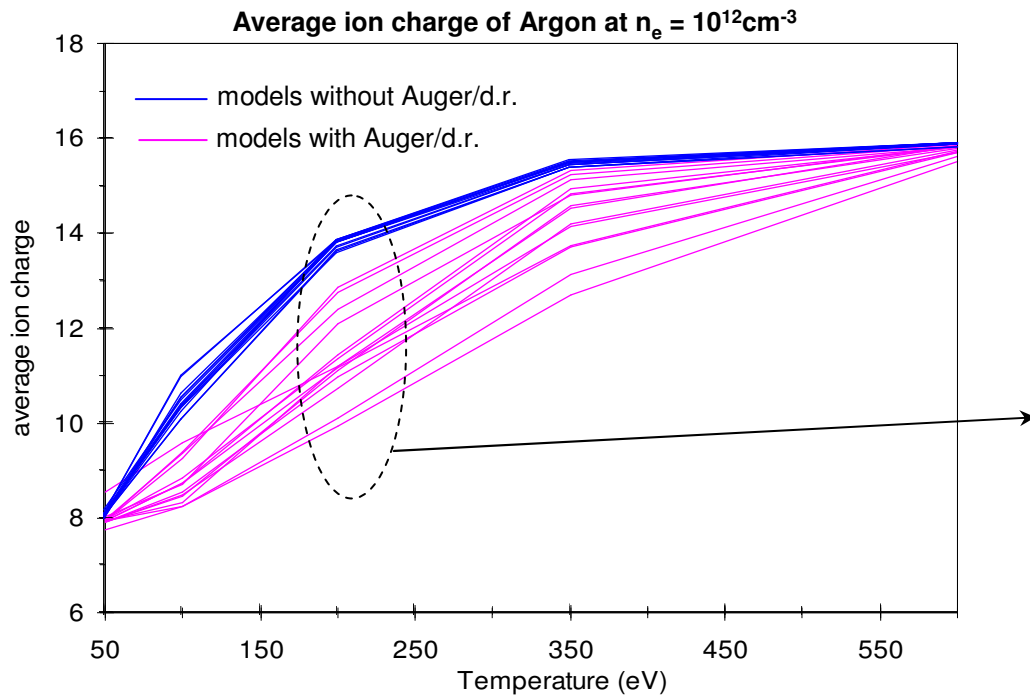
Example:
L-shell Au emission
from LLNL EBIT [1]



Low-density emission spectra are well-modeled by fine-structure models with only singly excited (coronal) states. Less accurate models generally do not capture the effects of metastable levels or configuration interaction.

Dielectronic recombination is critical for accurate collisional-radiative modeling

Recent non-LTE workshop results illustrate the importance of d.r.
– and the challenge of getting it right.

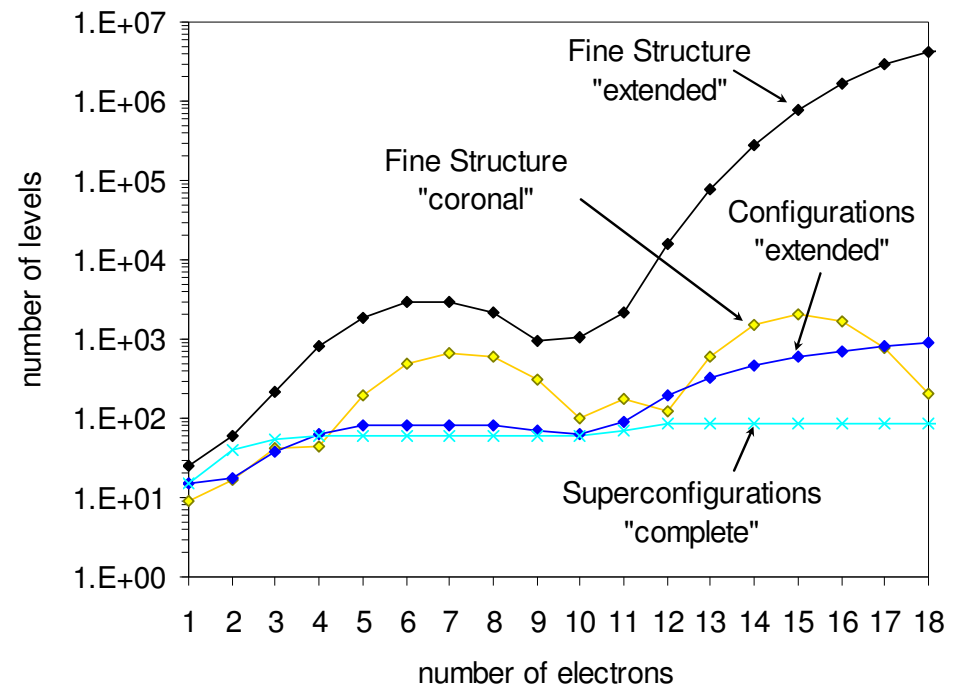


For coronal plasmas, global d.r. rates can be used (e.g. Mazotta [2], Bryans [3]), but these do not guarantee accurate satellite emission and are not valid at high densities.

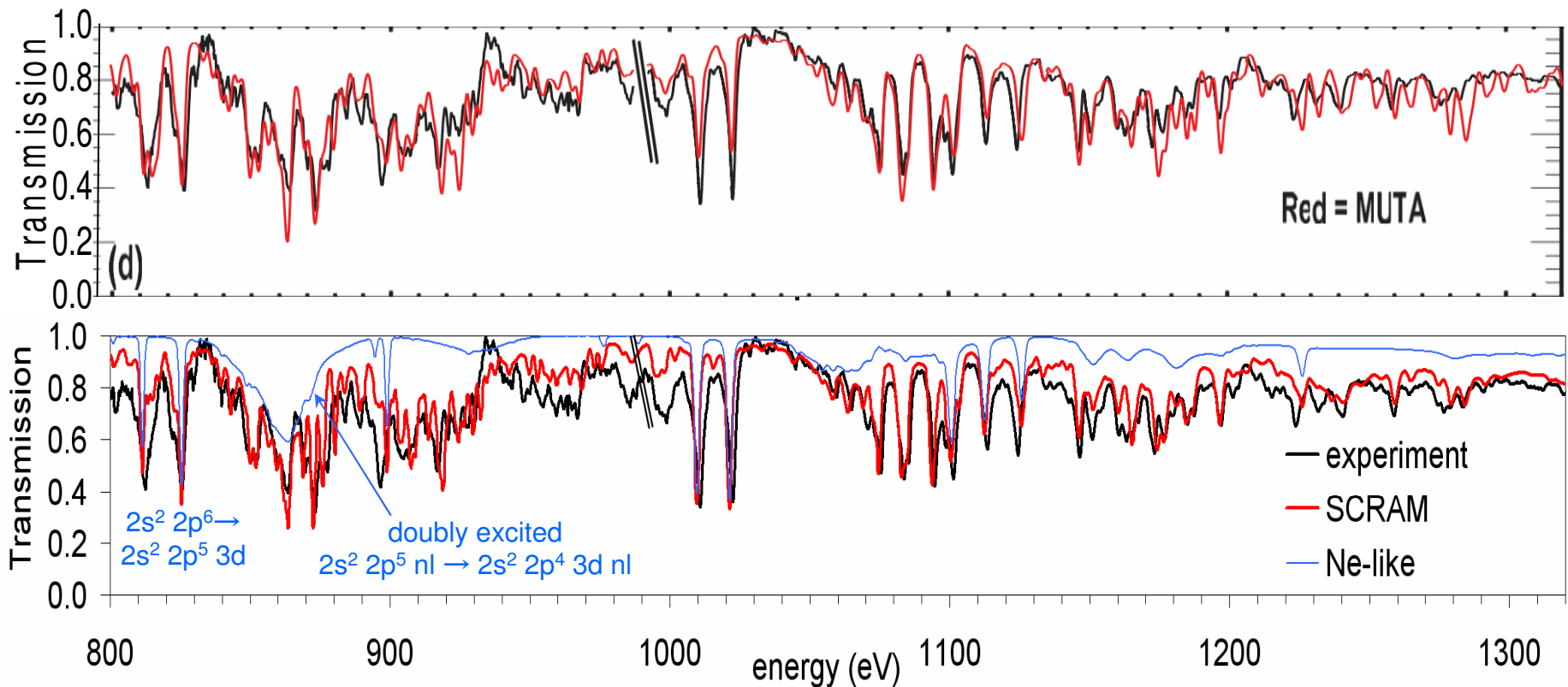
For complex ions, extensive fine structure models become intractable

While the number of singly-excited, “coronal” levels remains reasonable with increasing ion complexity, the number of levels required for an extensive model grows exponentially.

However, only “complete” models with extensive multiply-excited structure can accurately account for dielectronic recombination and satellite emission.



Heroic modeling efforts can give excellent agreement with high-density experimental data



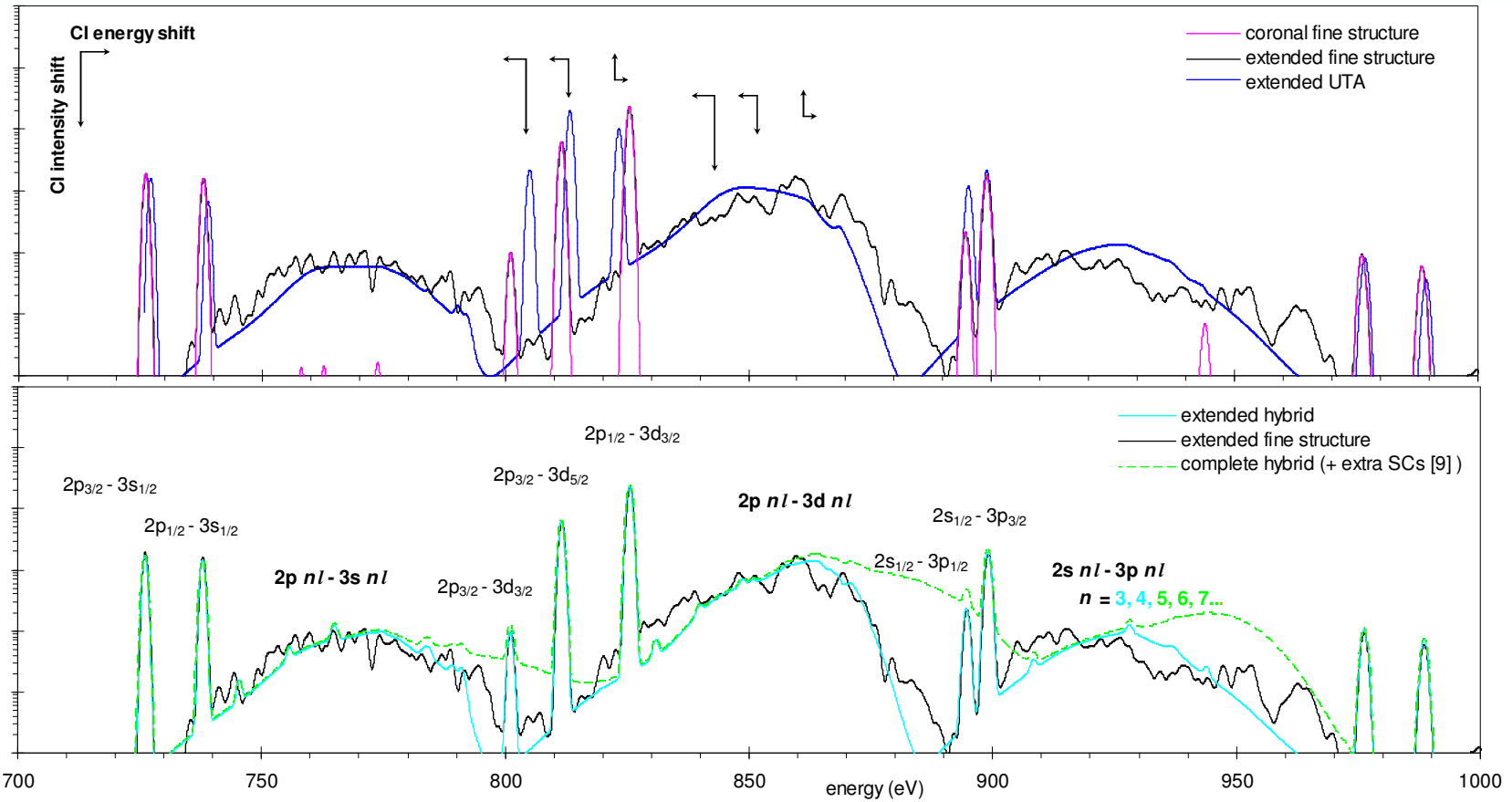
LANL's MUTA [4], a huge fine-structure model with more than 10^7 transitions (some averaged) matches measured Fe L-shell transmission [5] very well, – as does a smaller hybrid-structure model [6].

[4] Mazevert and Abdallah, J. Phys. B **39**, 3419 (2006)

[5] Bailey *et al.* PRL **99**, 265002 (2007)

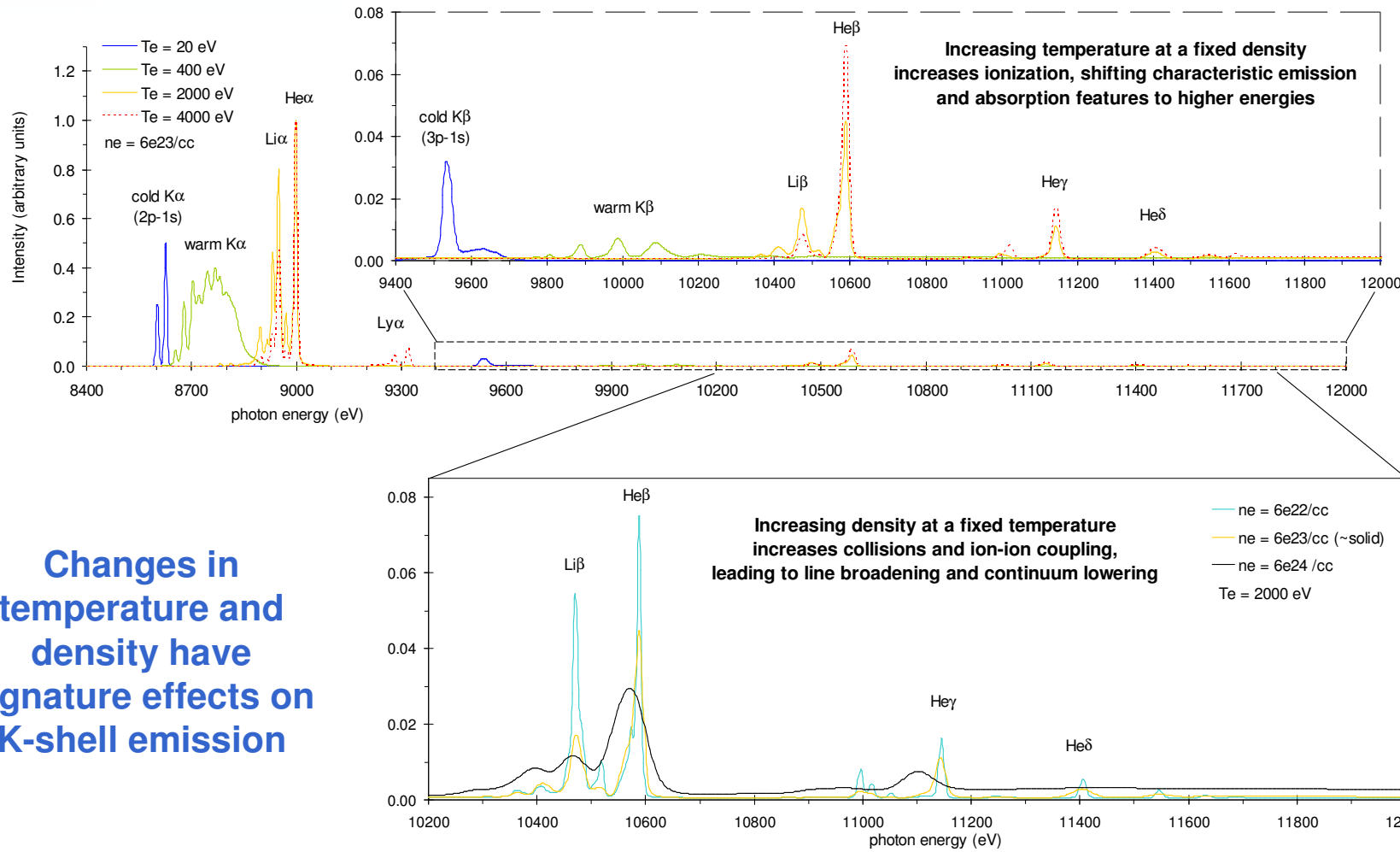
[6] Hansen *et al.*, HEDP **3**, 109 (2007)

Extending configuration interaction (CI) from fine structure transitions to UTAs is key



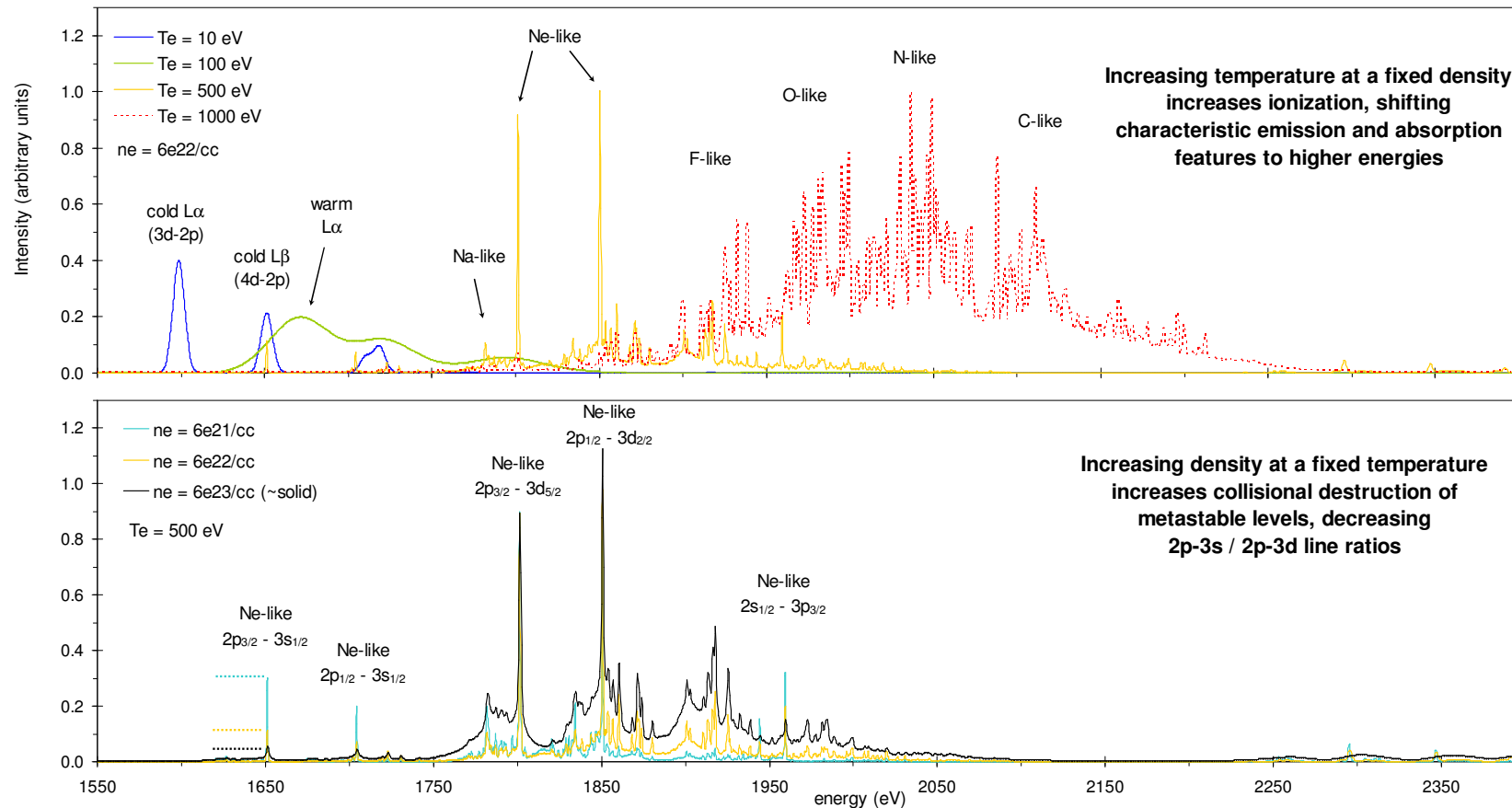
Each $nlj - nlj$ transition in each ion has its own CI corrections obtained from the overlapping sets of fine structure transitions and UTAs [1]

K-shell spectra are the traditional workhorses of spectroscopic plasma diagnostics



Changes in temperature and density have signature effects on K-shell emission

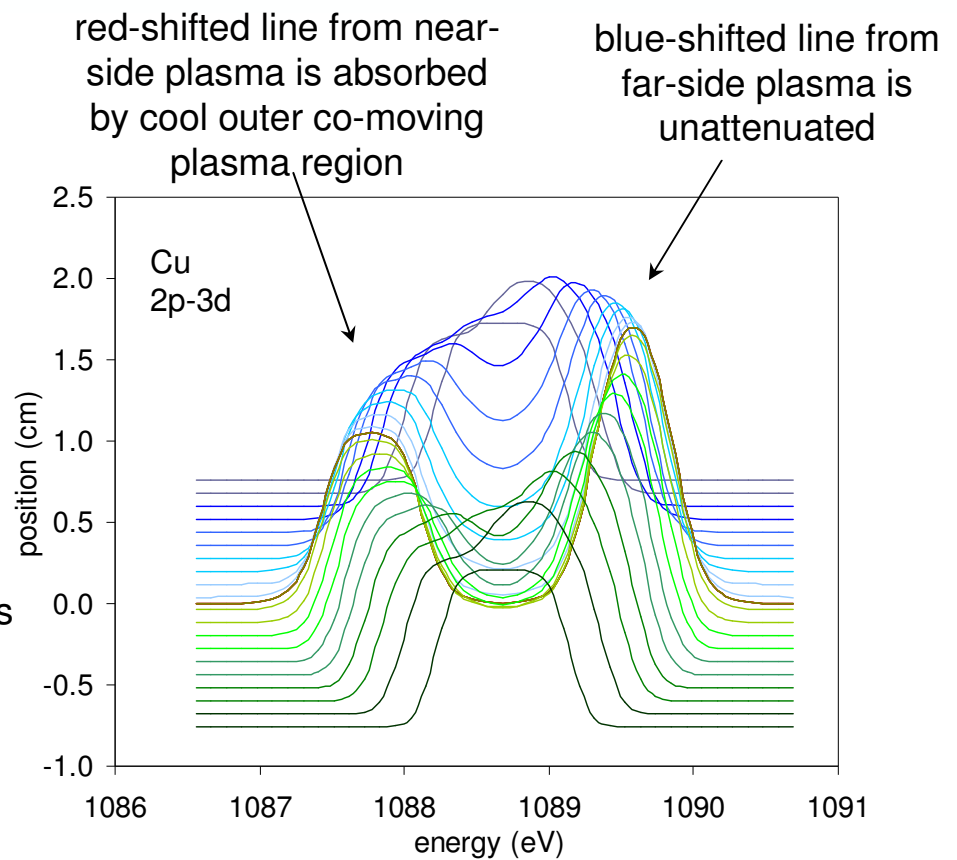
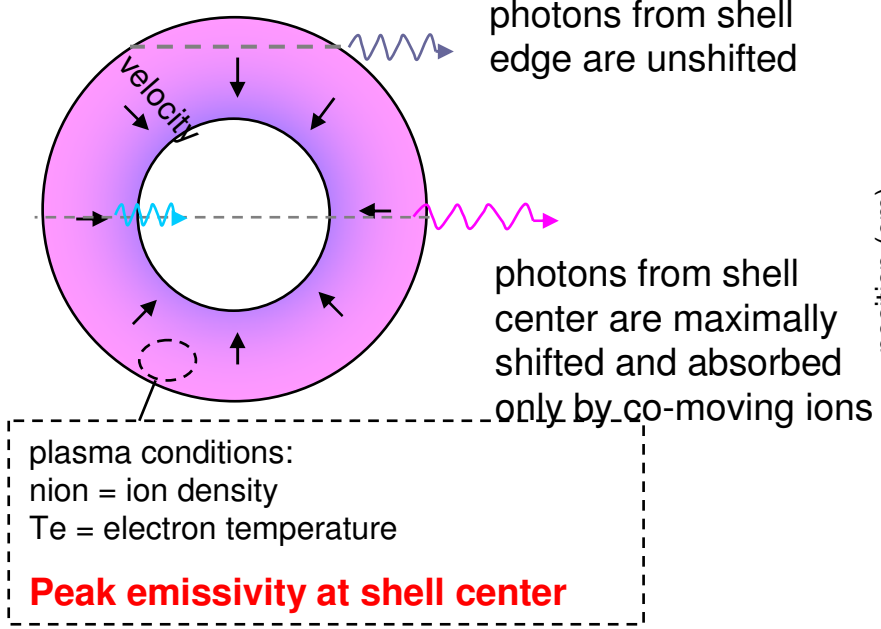
Reliable hybrid models offer new diagnostic opportunities with L-shell spectra



L-shell diagnostics have attractive features including unambiguous temperature dependence and resolution-independent density sensitivity

Self-consistent radiation transport is important for optically thick plasmas

Imploding Cu plasma shell

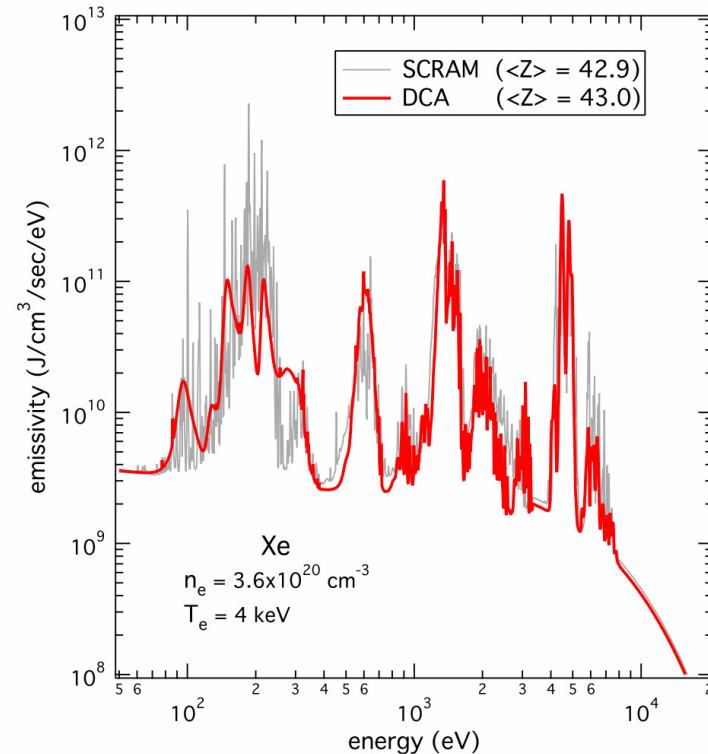


Opacity effects can lead to complex signatures in radially resolved spectral lines (c.f. Jones, Maron, *et al.*)

Accurate non-LTE models benchmark the fast in-line models used in radiation-hydrodynamics simulations

Most in-line radiation transport in multi-dimensional models has limited spectral resolution (“groups”) so spectroscopic accuracy is not required. However, *completeness* is necessary for reliable $\langle Z \rangle$, power losses, and opacities.

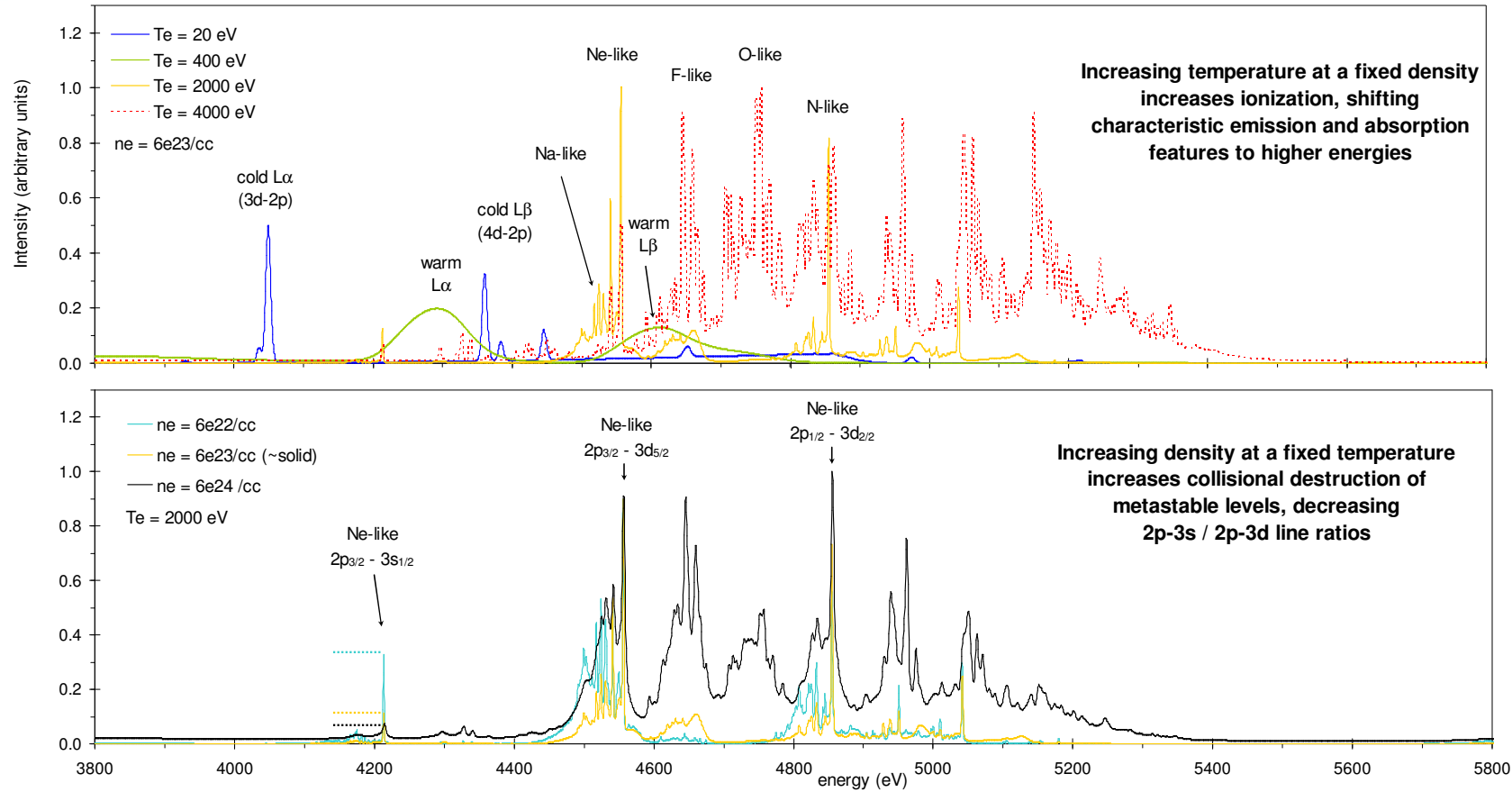
Spectroscopic-quality hybrid models with ~ 3 - 60 min runtimes can be used to benchmark the faster models (e.g. DCA [9]) used in radiation-hydrodynamic codes.



Computational constraints in multi-D rad-hydro limit atomic model runtimes to ~ 1 second!

[9] Scott and Hansen, HEDP 6, 39 (2010)

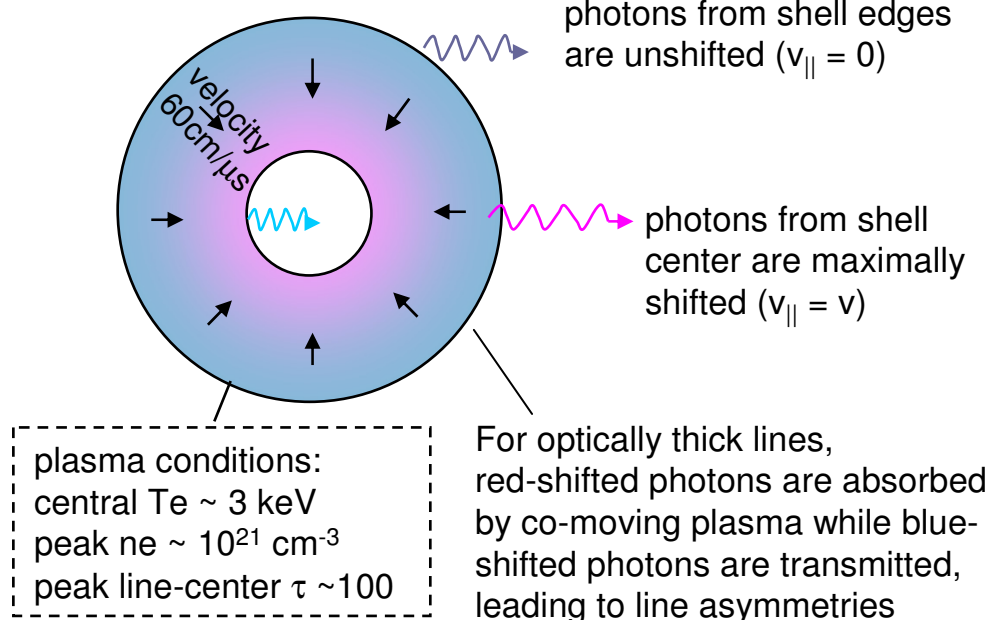
Reliable hybrid models offer new diagnostic opportunities with L-shell spectra



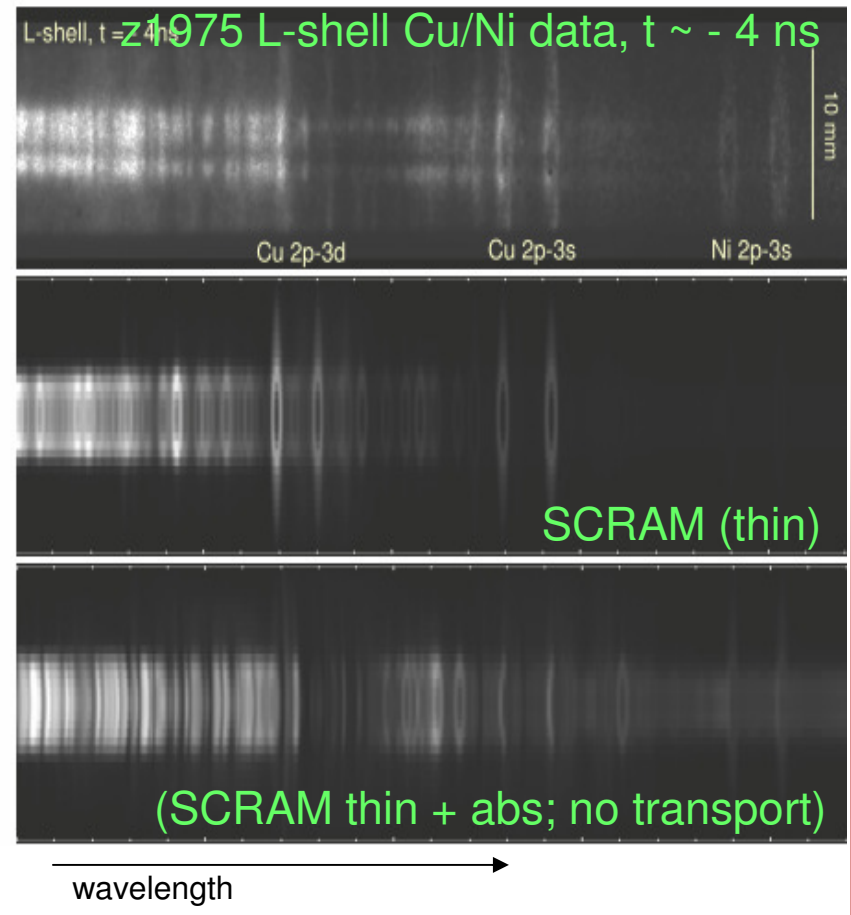
L-shell diagnostics have attractive features including unambiguous temperature dependence and resolution-independent density sensitivity

Temporally and spatially resolved spectra contain a wealth of information about the emitting plasma

Imploding Cu/Ni plasma shell
brightest on inner edge

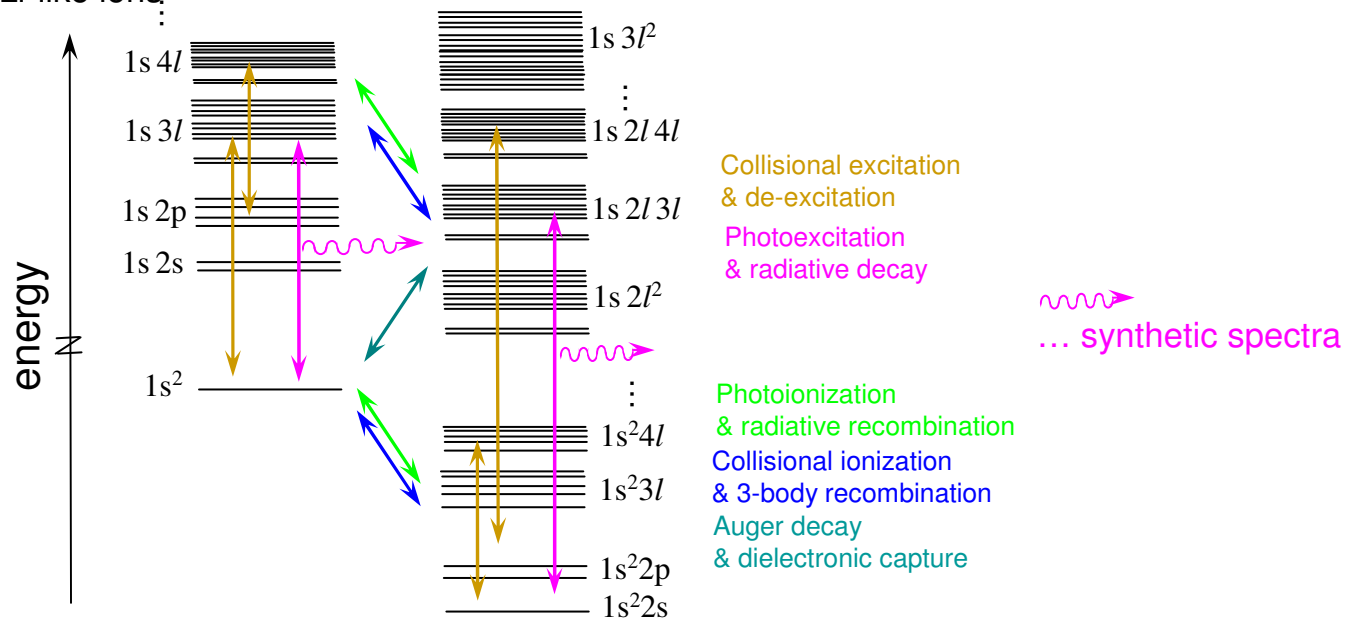


Reliable atomic models and self-consistent radiative transport are both essential for modeling optically thick emission from complex plasmas.



Reliable atomic models require complete level structure and accurate atomic data

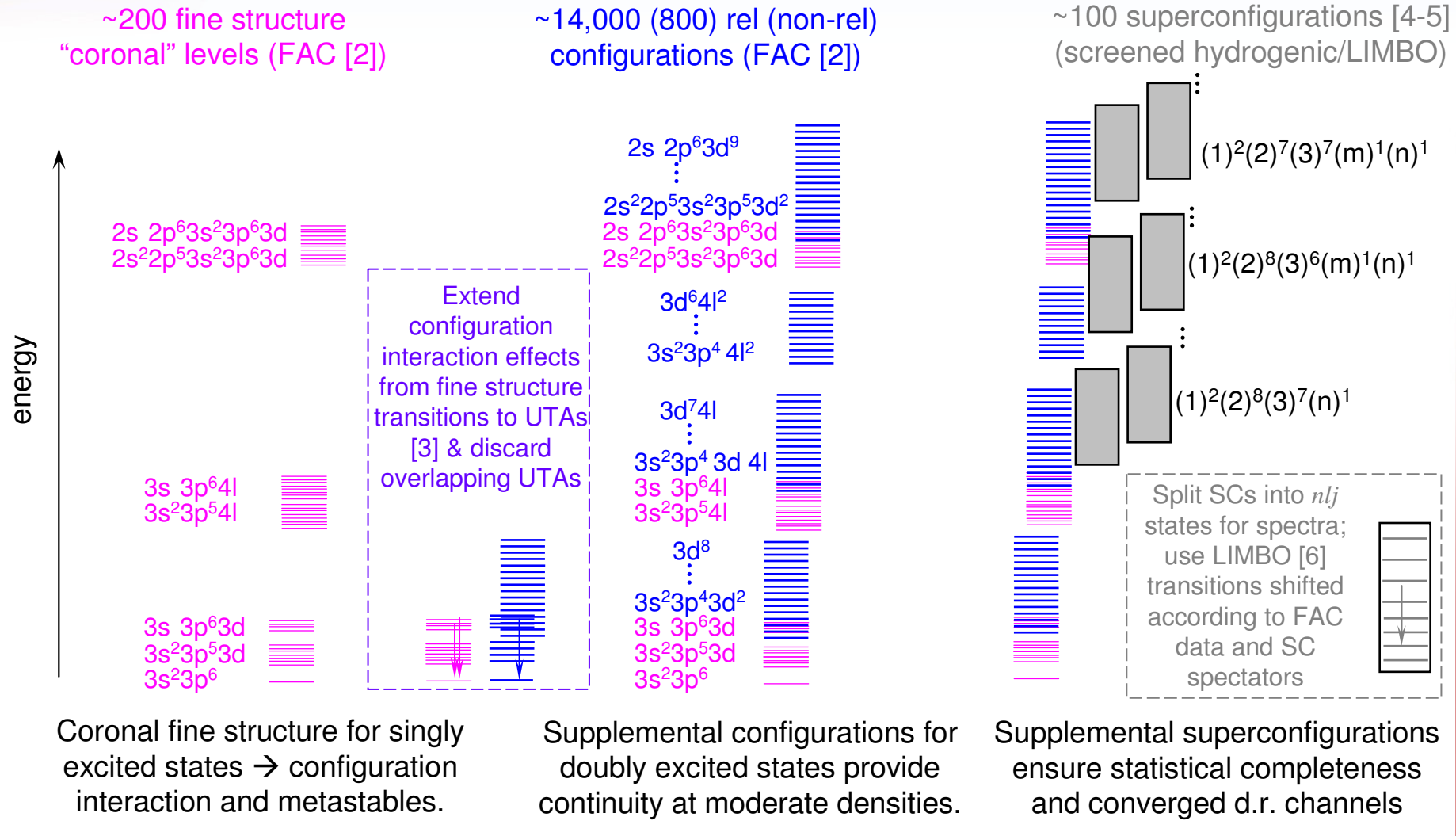
Example: He- and Li-like ions



A variety of codes, (RATS, FAC, Cowan...), databases, (NIST, ATOMDB...), and approximations (screened hydrogenic, Lotz...) provide energy level structure and rate data – with various degrees of detail and accuracy.

Generally, only fine structure data includes the configuration interaction effects and detailed transition structure required for spectroscopic accuracy... but fully fine structure models are computationally intractable for complex ions.

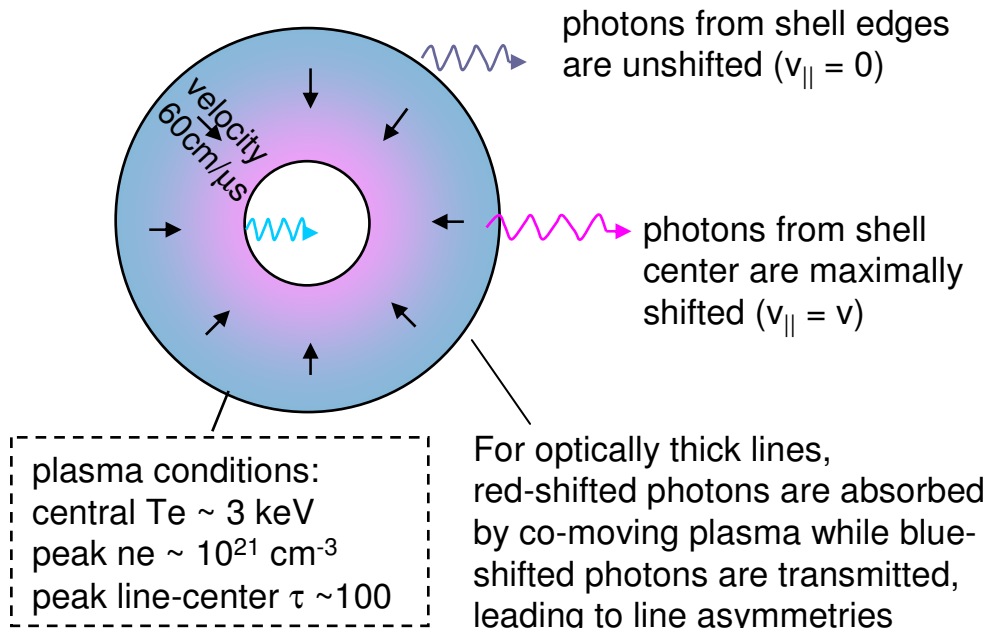
A hybrid-structure approach [1] combines the strengths of fine-structure and UTA/SC models



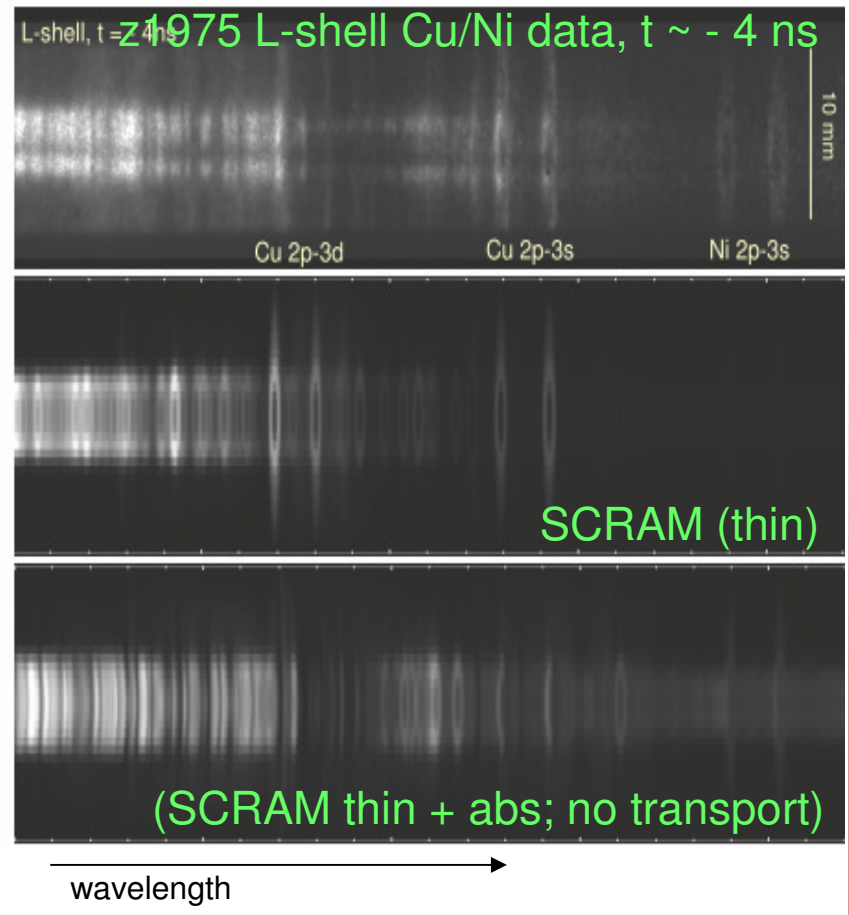
[1] Hansen, Bauche, Bauche-Arnoult, and Gu, HEDP 3, 109 (2007)
 [2] Gu, Astrophys. J. 590 1131 (2003)
 [3] Hansen, Can. J. Phys. 89 (2011)

[4] Scott and Hansen, HEDP 6, 39, (2010)
 [5] Hansen, Bauche, and Bauche-Arnoult HEDP 7, 27 (2010)
 [6] Liberman, Albritton, Wilson, & Alley, Phys. Rev. A 50, 171 (1994)

Accurate 0-D atomic models are not sufficient to model optically thick lines in complex plasmas



Including line absorption while neglecting transport photopumping is worse than treating an optically thick NLTE plasma as optically thin.



Approximate self-consistency is relatively straightforward for uniform, static plasmas

Self-consistent methods with analytical frequency-integrated escape factors P_{esc} [1,2] can be used for arbitrary geometries. They converge quickly but neglect line overlap.

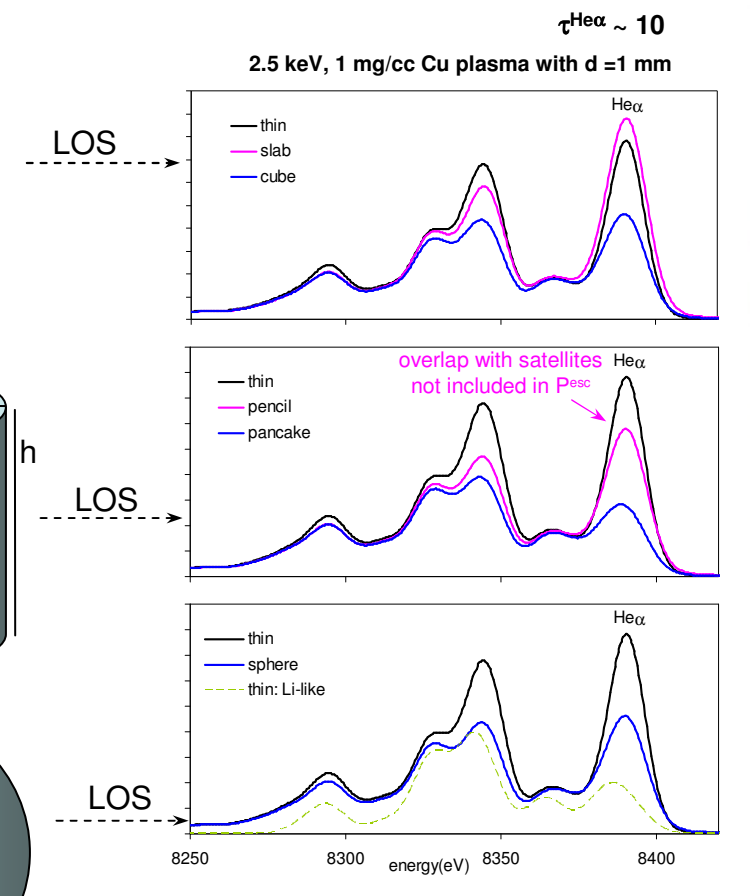
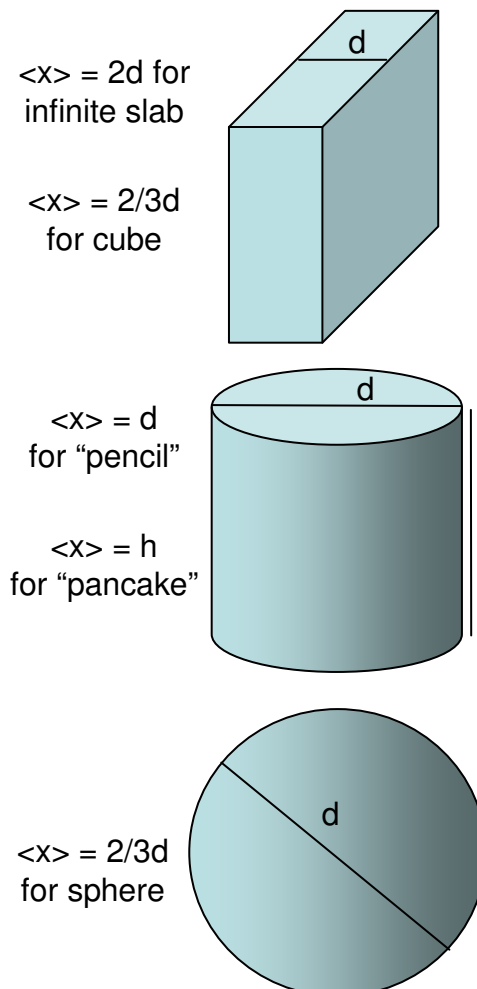
The effects of photoexcitation in a regular solid depend on the mean chord $\langle x \rangle$, while photoabsorption depends on the line of sight [3]

Self-consistent level populations: multiply A^{rad} & R^{rad} by $P_{\text{esc}}(\kappa \langle x \rangle)$

Emission profiles:
 $I = j/\kappa(1 - e^{-\tau})$; $\tau = \kappa x^{\text{LOS}}$

Photoabsorption along x^{LOS} can be larger or smaller than photoexcitation across $\langle x \rangle$

Neglect of satellites can lead to $\sim 30\%$ error



- [1] J.P. Apruzese JQSRT **23**, 479 (1980)
- [2] J.P. Apruzese JQSRT **25**, 419 (1981)
- [3] G.J. Phillips *et al.*, HEDP **4**, 18 (2008)

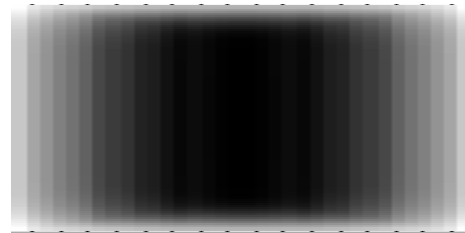
Even with uniform plasma conditions, level populations vary in space

Consider uniform cylindrical plasmas with two-level atoms; the geometry is defined by axial and radial optical depths and the source function is determined by non-local transport.

“Pinhole” images of the emission intensity from two cylindrical plasmas:



$\tau_0^{\text{axial}} = 50$
 $\tau_0^{\text{radial}} = 5$

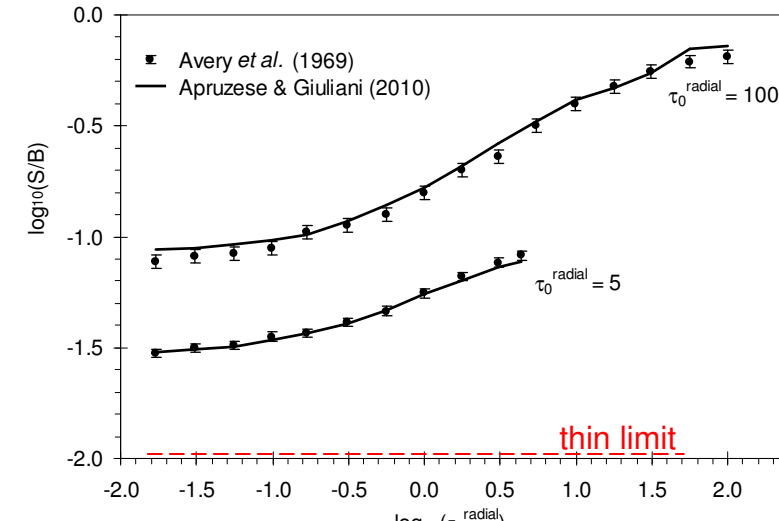
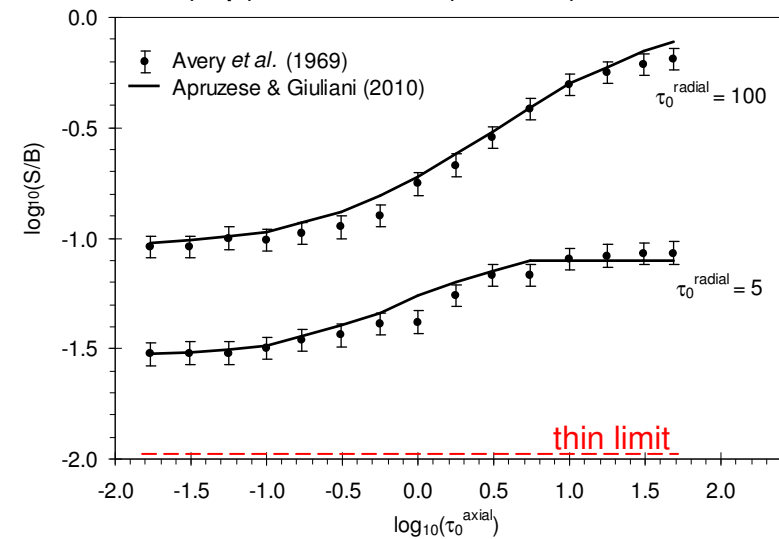


$\tau_0^{\text{axial}} = 50$
 $\tau_0^{\text{radial}} = 100$

Monte Carlo [2], multi-frequency, and non-local escape factor methods [1] all predict significant global photopumping from the thin limit of $\log_{10}(S/B) = -2$, with the highest intensities at plasma center.

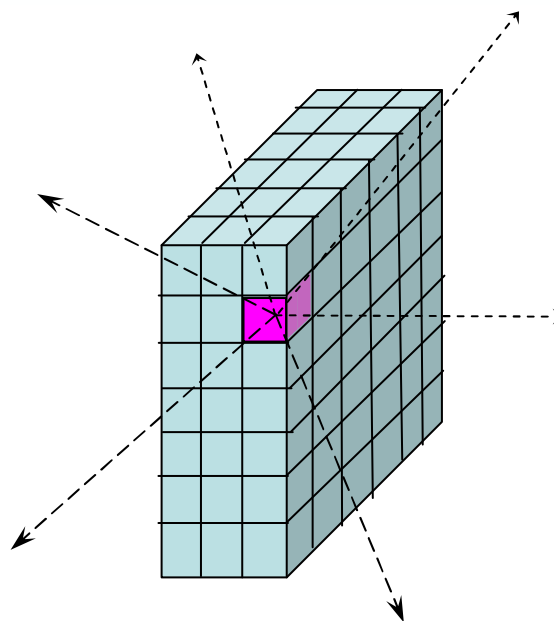
[1] Apruzese & Giuliani, JQSRT 111, 134 (2010)
[2] Avery *et al.*, JQSRT 9, 519 (1969)

Axial (top) and radial (bottom) emissivities:



On-the-spot approximation [1] can approximately account for bulk photoexcitation

- 1) Tabulate emissivities and opacities from self-consistent escape factor models on grids of T_e , n_{ion} , and plasma size (τ^{eff})
- 2) Determine frequency-averaged escape factors $P^e = \int_v j(v) e^{-\tau} dv / \int_v j(v) dv$ along various lines of sight (8 – 14 rays) and find angle average $\langle \tau^{eff} \rangle \equiv -\ln(\langle P^e \rangle_\Omega)$ for each plasma element
- 3) Set $j(v)$ of each plasma element to the tabulated $j(v)$ of the self-consistent model with $\tau^{eff} = \langle \tau^{eff} \rangle$ (+ symmetry speedup)
- 4) Transport emissivity to detector along instrumental line of sight

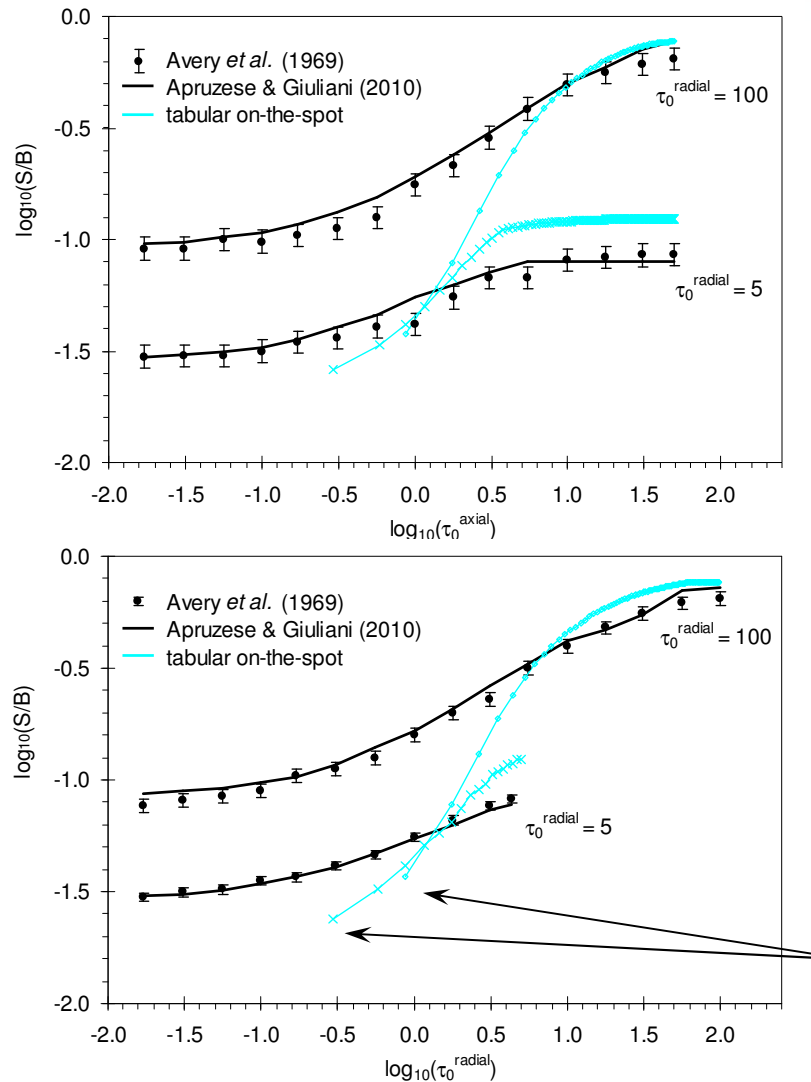


Key approximations:

- all absorbed photons are returned to originating cell (partially local transport)
- self-consistency is enforced only by table (no iteration on plasma grid)
- opacity is dependent only on T_e & n_{ion}
- escape factor method has its own inaccuracies

[1] Thornhill *et al.*, Phys. Plas. 8, 3480 (2001)

On-the-spot method does not accurately capture non-local transport effects



- + The on-the-spot method is explicitly photon conserving and accounts for the bulk effects of photopumping on the total line intensity.
- + It also captures the trend of increasing intensities with optical depth.
- + Tabular and analytic ($S/B = (1+P^e/\epsilon)^{-1}$) on-the-spot methods agree.
- However, because the edge cells will never have $\langle P^e \rangle_\Omega$ smaller than ~ 0.5 , the method under-predicts edge intensities and over-predicts intensities at line center (photons emitted from the center are absorbed at the center, rather than transported to the plasma edge)

Minimum τ is enforced by cell size
(linear grids require $\sim 10^6$ cells)

Weighting the escape probabilities and iterating significantly improves the on-the-spot method

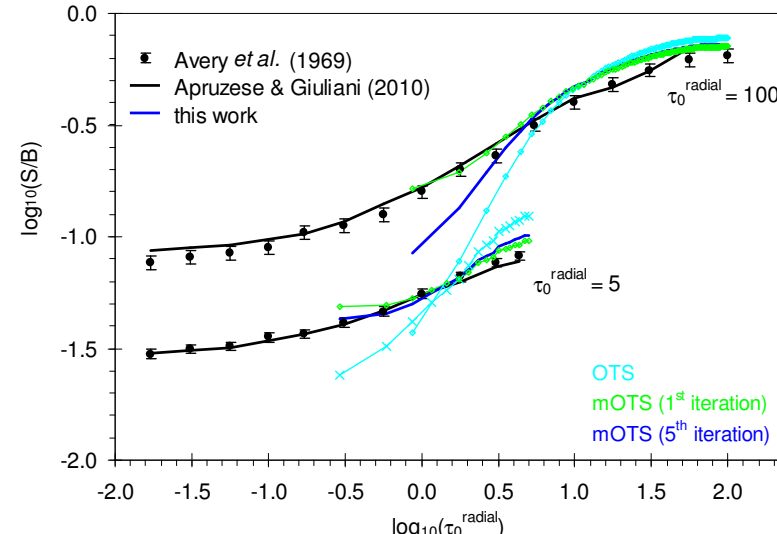
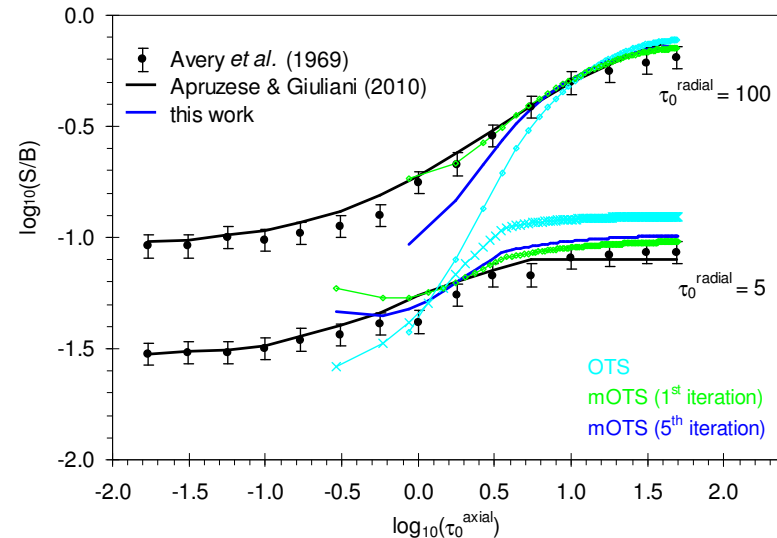
Instead of weighting angles equally, weight according to the total intensity incident on the cell along each ray:

$$w \sim \sum_k \int_v j_k(v) e^{-\sum \tau_k} dv$$

Then normalize the total final intensity to that of the initial on-the-spot iteration to conserve photons.

Convergence to $\sim 1\%$ percent is reached in ~ 5 iterations.

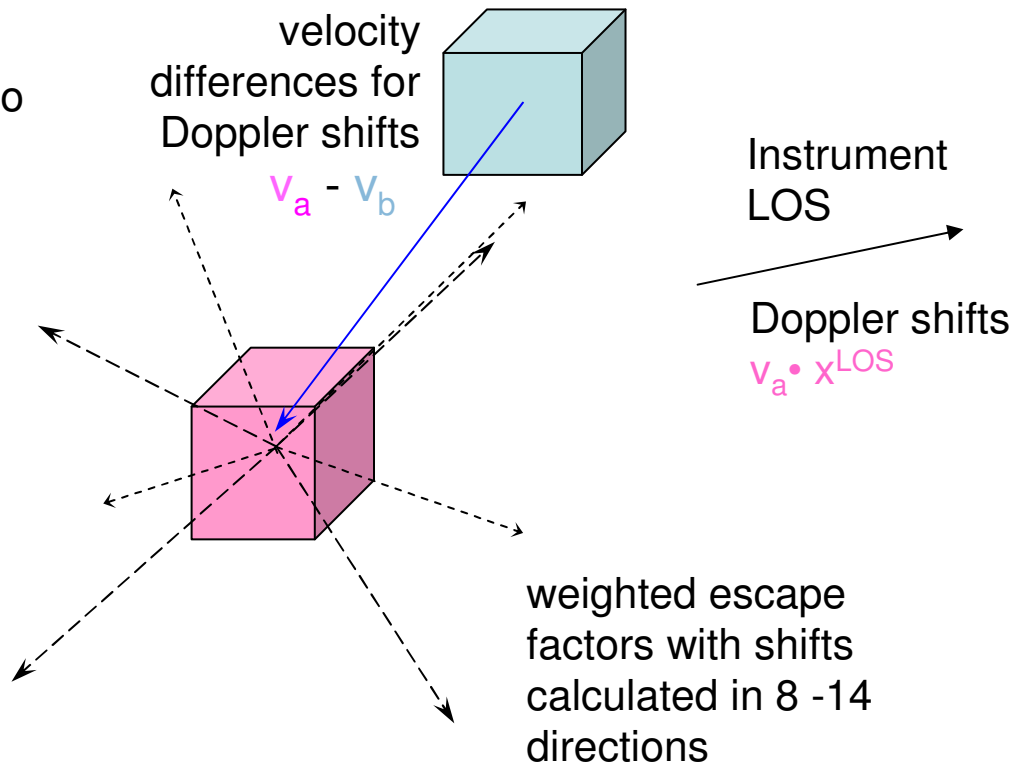
This iterative approach captures more of the non-local transport behavior and better matches the more sophisticated models.



The modified OTS transport model handles complex geometries, spectra, and Doppler shifts

Eulerian grid & tabular approach has conceptual and computational advantages:

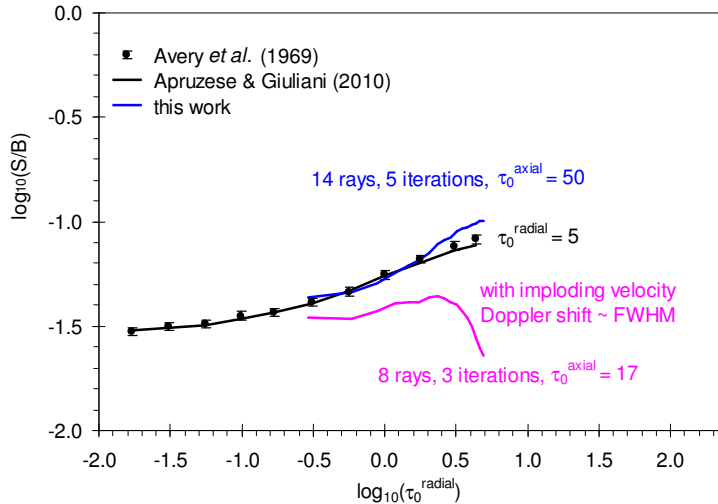
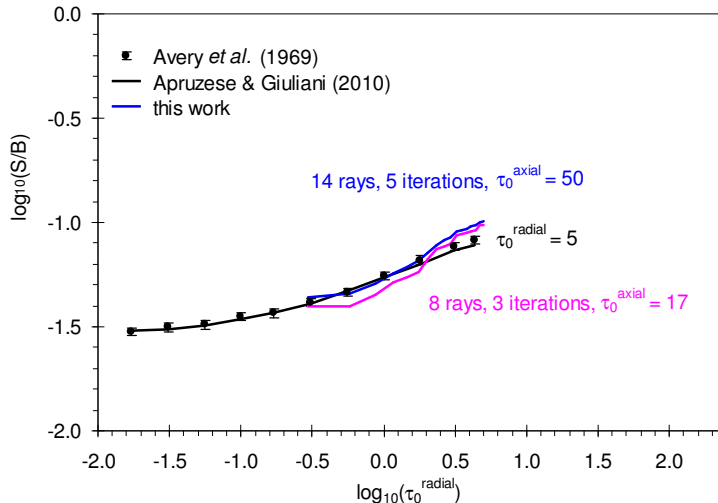
- 1) Tabulated spectra are calculated once for each element for cubes with $\tau_{\max} \sim 0.3$ to ~ 300 (for $h\nu = 200 - 20$ keV on 3×10^4 frequency points!) then mixed & interpolated for custom materials
- 2) 1D and 2D plasma geometries can be spherically or cylindrically symmetrized for significant computational savings, but full 3D is possible
- 3) Rays for angle-averaged escape factors are taken from cube center to cube corners; velocity vectors can be mapped once to these rays and to instrumental line of sight
- 4) Fast convergence (~ 10 min for 10^5 cells, fully 3D)



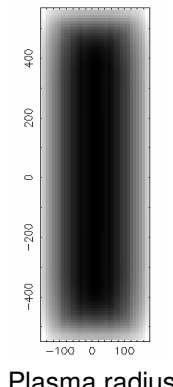
The transport model was developed with GORGON, a 3D Eulerian Cartesian code, in mind. Handshakes with this and other codes are under development.

Including Doppler effects reduces photopumping and changes line profiles

Radial source functions:
no Doppler (top) & with Doppler (bottom)

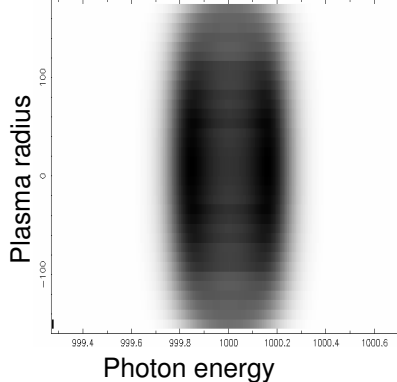


$\tau_0^{\text{axial}} = 17$
 $\tau_0^{\text{radial}} = 5$

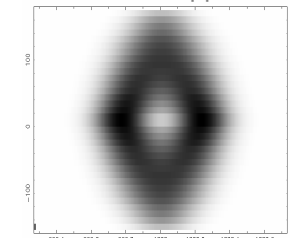


Radially resolved spectra

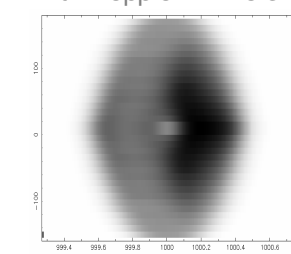
No Doppler in transport
No Doppler in line or absorption



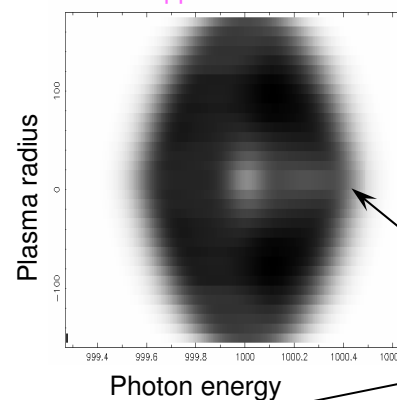
No Doppler in transport
THIN with Doppler in line



No Doppler in transport
With Doppler in line & abs.



With Doppler in transport
With Doppler in line & absorption



“hollow” core
& asymmetric line

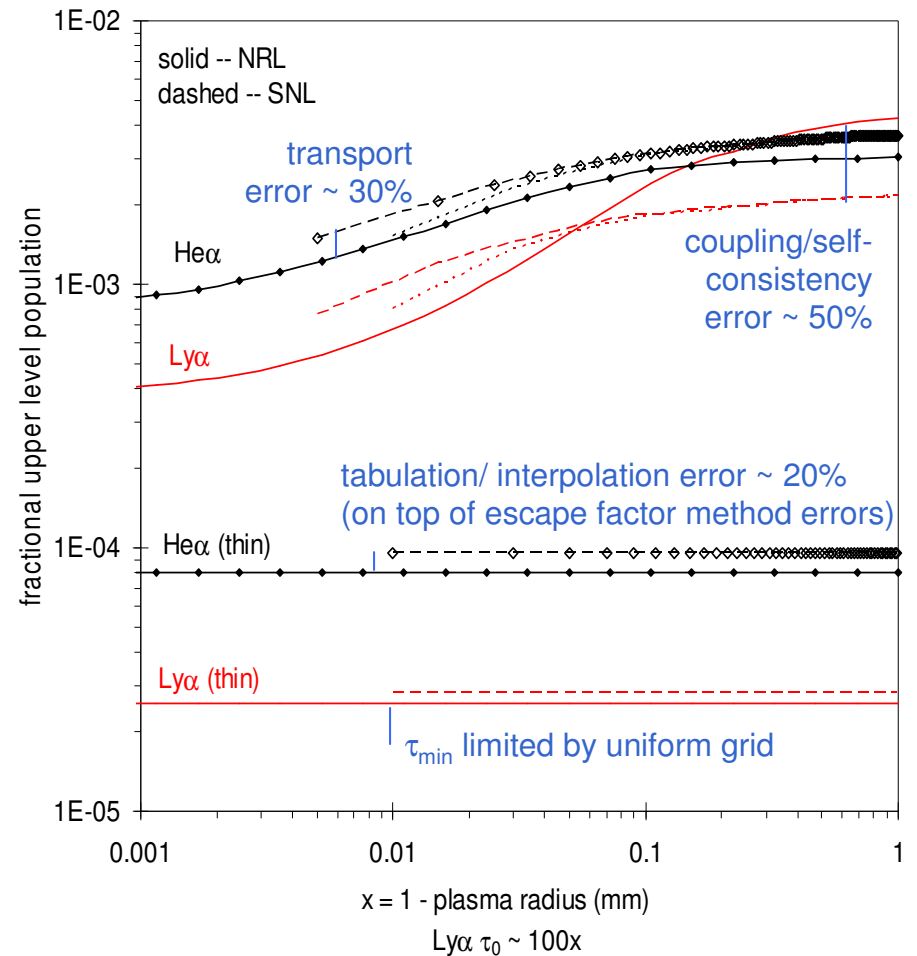
Additional comparisons that more stringently test the transport model are underway

In collaboration with NRL, we have defined an 8-level model of H- and He-like Al and performed calculations for a cylindrical plasma ($T_e = 0.5$ keV, $n_{ion} = 10^{20}/cc$, $h = 20$ mm, $r = 1$ mm) see J. P. Apruzese talk this afternoon

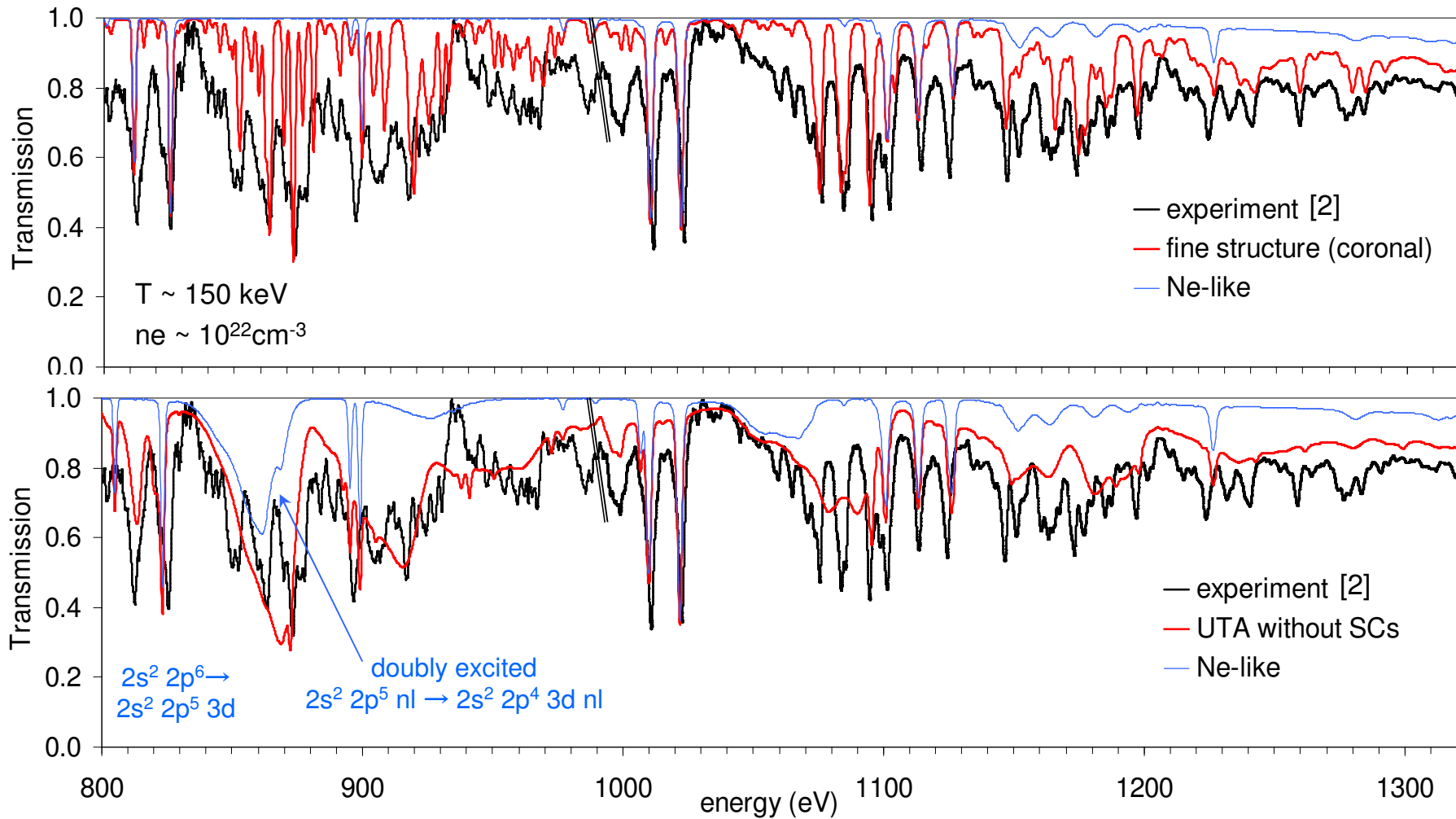
NRL computes full multi-angle, multi-frequency transport for each line and performs fully self-consistent coupling of transported photons and level populations.

Comparisons with the modified tabular on-the-spot approach reveal consequences of various approximations: spatial gridding, spectral tabulation, transport method, and coupling consistency.

Despite these limitations, the approximate model produces reasonable results for bulk photopumping and emergent lineshapes.



Extensive level structure is critical for high-density absorption spectra

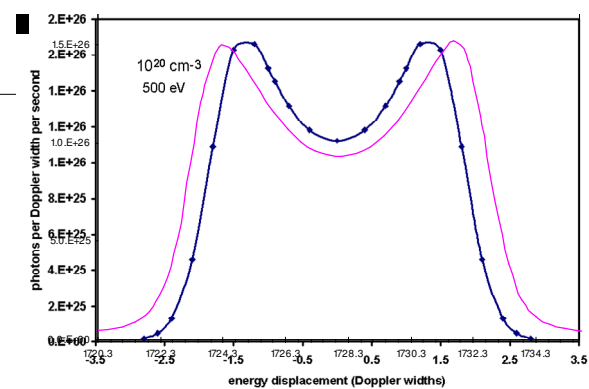
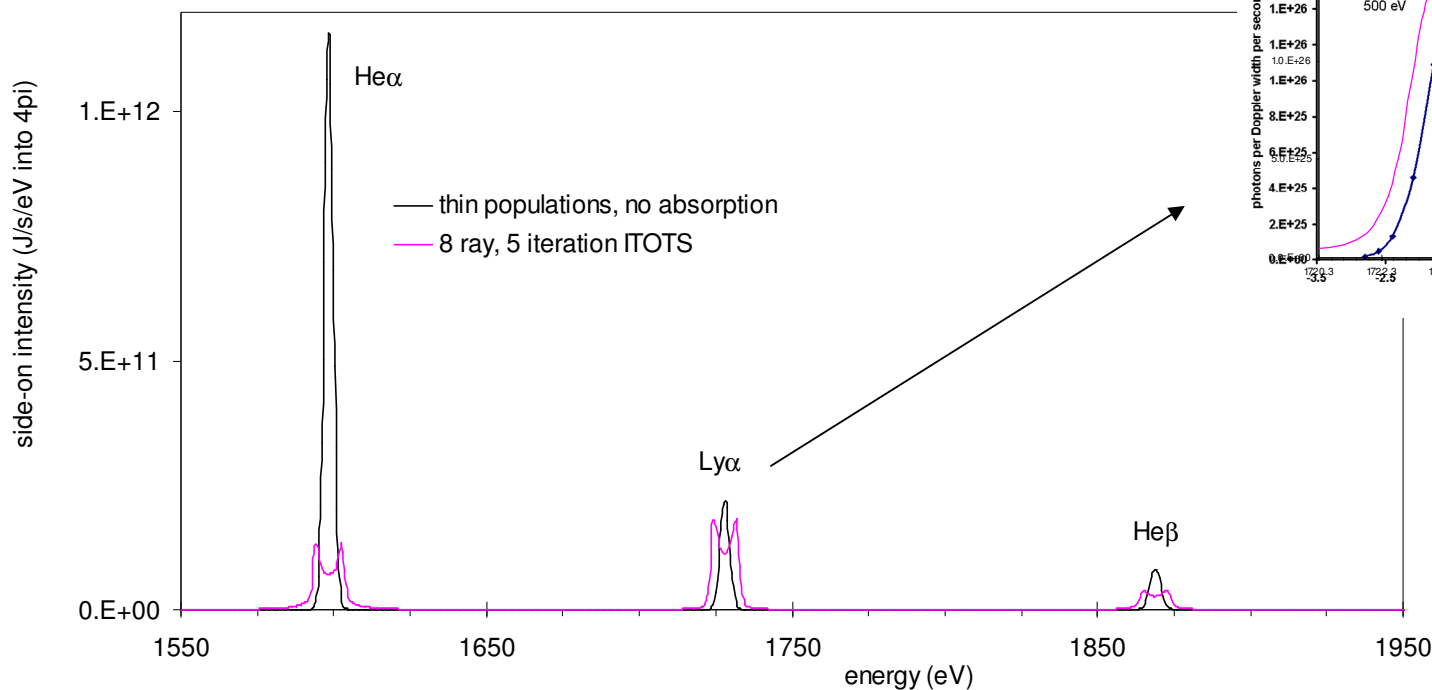


UTA model with extensive structure reproduces overall absorption
but misses detailed features

[2] Bailey *et al.* PRL **99**, 265002 (2007).

Despite these weaknesses, the approximate method gives reasonable line shapes and intensities

Photopumping and opacity effects significantly alter relative intensities:



NRL and SNL Ly α line profiles show strong line-center absorption and are in reasonable agreement